

Fig. 3. Quantitative verification of kinetics of association and dissociation of phagosome proteins. (A) Immunoblots of 10 µg of the phagosome samples prepared at various time intervals (chase 0–120 min) and total crude lysate (TL). Proteins were electrophoresed on SDS–polyacrylamide gel, blotted to a nitrocellulose membrane, and reacted with specific antibodies against Igl, Rab11B, Rab7A, Rab7E, Lgl, and CP5. (B) The relative amount of each protein was measured by chemiluminescence detection of immunoblots (solid lines) and plotted together with the results of percentage coverages based on MS analyses (dotted lines).

detected peptides per protein are influenced by several factors including the relative protein abundance, the size of whole proteins, and the number of the trypsin cleavage sites, we confirmed the mass spectrometry data of representative proteins involved in surface recognition, vesicular trafficking, and protein degradation by quantitative immunoblots. These quantitative analyses (Fig. 3A and B, unbroken lines) agreed well with the coverage data by MS analysis, indicating that the changes in the peptide coverages during phagosome maturation truly reflect changes in the relative abundance of individual phagosome proteins.

3.5. Verification of time-specific recruitment and dissociation of phagosome proteins

We directly verified the kinetics of phagosome recruitment, which was suggested by MS and quantitative immunoblot analyses, using video microscopy of live amebas. An ameba transformant expressing GFP-*EhRab7A* was used to examine dynamic association and dissociation of *EhRab7A*. The live transformant was examined every 1 min for 120 min after internalization of a single bead. Live video microscopy demonstrated that GFP-*EhRab7A* was first detected on a phagosome at 2 ± 0.7 (mean \pm standard deviation, $n=4-5$) min after the bead internalization (an only representative image at 5 min is shown in Fig. 4). GFP-*EhRab7A* was dissociated from the phagosome at 26 ± 4.4 min and the phagosome remained devoid of GFP-*EhRab7A* until 56 ± 9.9 min (Fig. 4, 30 min). GFP-*EhRab7A* was recruited again (Fig. 4, 60 min) and remained associated with the phagosome (Fig. 4, 120 min). Although the dynamism of an only representative cell is shown, at least five other cells showed comparable kinetics. The direct demonstration of association to and dissociation from phagosomes of GFP-*EhRab7A* reinforces the kinetics of *EhRab7A* demonstrated with proteomic analysis. We previously showed that *EhRab7A* was recruited to and localized in phagosomes between 5 and 20 min after incubation with red blood cells and was then dissociated from phagosomes at 30–50 min [24]. Thus, although the kinetics of *EhRab7A* was not shown after 50 min of erythrocyte ingestion, the kinetics of *EhRab7A* shown in the present study is consistent with our previous observation. We also examined the control transformant expressing GFP, but GFP was not recruited to phagosomes during the formation and maturation of phagosomes as previously shown [26].

3.6. Comparison of phagosome protein profiles among three *E. histolytica* strains

Since it has been previously shown that clinical isolates are genetically polymorphic [11,39], we examined variation of the phagosome protein profiles among three *E. histolytica* strains: HM1 and two recent clinical isolates (KU33 and HATAJI). Phagosomes were isolated from these strains at 0 and 30 min and analyzed by LC-MS and MS/MS under the identical conditions. Peptide sequences of a total of 2866 and 2717 peptides (300–1000 peptides per sample) were obtained from biological duplicate samples of two time points in KU33 and HATAJI, respectively, and unequivocally assigned to 117 and 116 pro-

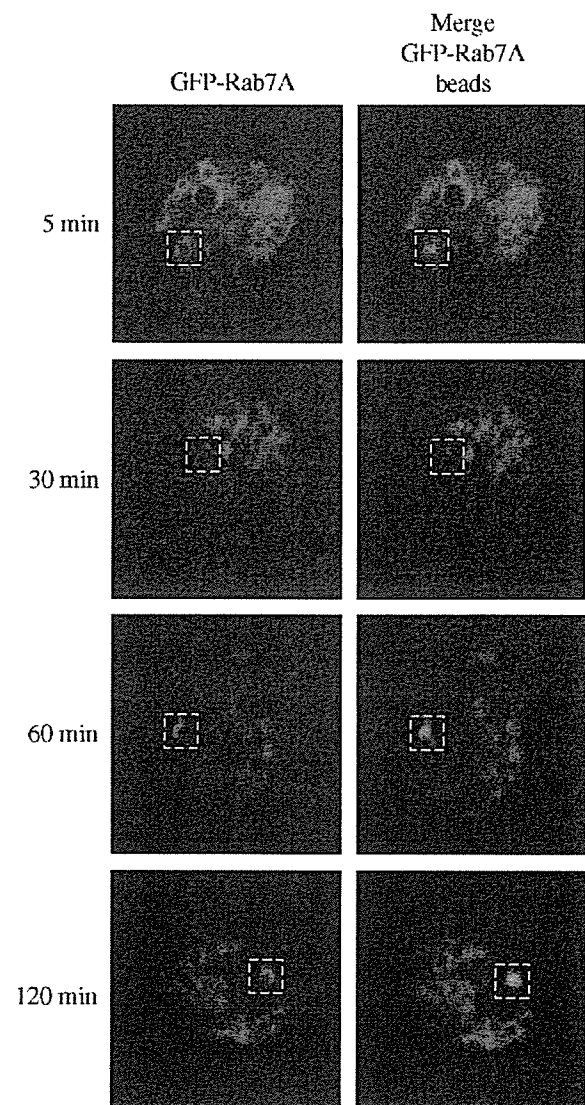


Fig. 4. Validation of the time-specific recruitment/dissociation of a representative phagosome protein by video microscopy. The dynamism of GFP-*EhRab7A* in the live GFP-*EhRab7A*-expressing transformant was examined after internalization of a single blue fluorescence-labeled bead for 120 min. Left and right panels show GFP-*EhRab7A* (green) and merged images of GFP-*EhRab7A* and a blue fluorescence bead (blue), respectively. Dotted squares depict the position of the internalized bead.

teins with the sequence coverage of 3–70% (KU33 and HATAJI, respectively). A comparison of these proteins identified in HM1, KU33, and HATAJI at combined two intervals (0 and 30 min after internalization of beads) is shown in Fig. 2B. When the proteins were compared among HM1, KU33, and HATAJI, 64% of proteins were detected only in a single strain, while 22% of proteins were identified in all three strains (Table 1, circles). Most of these proteins identified in all three strains (67%) were constitutively detected in phagosomes from HM1. Table 2 shows 52 phagosome proteins detected only in either KU33 or HATAJI, or both, but not in HM1. Together with 32 hypothetical proteins (Supplementary Table S2), these 84 out of 229 proteins

Table 2
Strain variations of phagosome proteins

TIGR protein ID	NCBI accession number	Protein name (organism source)	Identity (%)	Chase (min)			
				KU33		HATAJI	
				0	30	0	30
Vesicular trafficking, other small GTPase, and effectors							
322.m00040	EAL43905	Adapter protein complex 2B 1 subunit (<i>Homo sapiens</i>)	54	±	–	±	±
116.m00130	EAL47110	Ras guanine nucleotide activating protein (<i>Gallus gallus</i>)	30	–	–	–	±
68.m00225	EAL48548	Ras guanine nucleotide activating protein (<i>Cryptococcus neoformans</i>)	29	–	–	–	±
172.m00077	EAL45904	Ras guanine nucleotide exchange factor 2 (<i>Homo sapiens</i>)	29	±	±	+	+
71.m00153	EAL48426	Rho ^a (<i>Anopheles gambiae</i>)	49	–	–	+	+
45.m00145	EAL49349	Rho guanine nucleotide activating protein ^a (<i>Dictyostelium discoideum</i>)	29	±	–	±	–
8.m00379	EAL51380	Rho guanine nucleotide exchange factor ^a (<i>Mus musculus</i>)	29	–	±	–	–
19.m00341	EAL50624	SNF7 (<i>Aspergillus fumigatus</i>)	32	+	+	+	+
Hydrolytic enzymes, digestive protein							
88.m00159	Q24824	Ameobapore B	100	+	–	–	–
69.m00164	EAL48510	Beta-amylase (<i>Oryza sativa</i>)	48	±	–	±	–
88.m00148	CAA60673	Cysteine protease 3	100	+	+	+	+
191.m00117	CAA62835	Cysteine protease 6	100	±	–	+	–
5.m00404	EAL51687	Exoribonuclease (<i>Arabidopsis thaliana</i>)	41	–	–	±	–
9.m00416	EAL51296	Invapore X (<i>Entamoeba invadens</i>)	69	–	+	–	–
103.m00185	AAO17820	Long iron-dependent hydrogenase 2 ^a	100	–	±	–	–
100.m00129	EAL47532	Ribonuclease t2 (<i>Cicer arietinum</i>)	29	+	+	–	–
177.m00126	EAL45818	Ribonuclease t2 (<i>Cicer arietinum</i>)	29	±	±	–	+
163.m00100	EAL46093	Ubiquitin-specific protease USP32 (<i>Homo sapiens</i>)	25	±	–	–	–
Cytoskeletal proteins							
98.m00144	EAL47592	Actin (<i>Candida boidinii</i>)	30	–	–	–	±
1.m00596	EAL52203	Actin-related protein 2 (<i>Dictyostelium discoideum</i>)	63	–	–	+	±
141.m00086	EAL46530	Coronin 7 (<i>Mus musculus</i>)	25	–	–	–	±
60.m00148	EAL48821	F-actin capping protein α subunit (<i>Dictyostelium discoideum</i>)	34	–	–	+	–
69.m00175	EAL48498	Formin dDia1 (<i>Dictyostelium discoideum</i>)	25	–	±	±	–
59.m00173	EAL48838	Villinin ^a (<i>Dictyostelium discoideum</i>)	25	–	–	±	–
Signal transduction							
207.m00072	EAL45251	fkbp-Rapamycin-associated protein (<i>Mus musculus</i>)	32	±	±	–	±
3.m00629	EAL51874	p41-Arc (<i>Dictyostelium discoideum</i>)	40	–	–	+	±
83.m00182	EAL48048	Phosphatidylinositol-3-kinase 2 (<i>Dictyostelium discoideum</i>)	37	–	±	–	–
6.m00490	EAL51587	Protein kinase (<i>Dictyostelium discoideum</i>)	32	±	–	–	–
150.m00109	EAL46348	Src Family kinase (<i>Asterina miniata</i>)	37	–	–	–	±
75.m00161	EAL48289	Tyrosine kinase protein (<i>Dictyostelium discoideum</i>)	29	–	±	–	–
Surface proteins							
324.m00038	EAL43893	ABC transporter protein 1 (<i>Leishmania major</i>)	45	±	±	–	–
302.m00042	EAL44054	Anion transporter 1 (<i>Mus musculus</i>)	30	±	–	–	–
Other proteins							
4.m00605	EAL51786	Cdc 45 (<i>Mus musculus</i>)	25	–	–	+	+
162.m00075	EAL46109	Condensin complex subunit (<i>Oryza sativa</i>)	33	±	±	±	±
118.m00154	EAL47035	Cortaxillin 2 (<i>Polysphondylium pallidum</i>)	37	±	–	+	–
33.m00212	EAL49854	Cyclase-associated protein homolog protein 1 (<i>Caenorhabditis elegans</i>)	30	±	±	±	–
223.m00079	EAL45000	Cysteinyl-tRNA synthetase (<i>Gallus gallus</i>)	40	–	±	–	–
78.m00158	EAL48193	Development and differentiation-enhancing factor 2 ^a (<i>Homo sapiens</i>)	25	±	–	–	–
206.m00081	EAL45255	DNA repair protein rad 18 ^a (<i>Schizosaccharomyces pombe</i>)	25	±	–	±	–
19.m00322	EAL50606	Ferric-chelate reductase (<i>Aspergillus fumigatus</i>)	25	±	±	+	+
213.m00081	EAL45154	Inositol polyphosphate-5-phosphatase (<i>Homo sapiens</i>)	29	–	–	±	–
66.m00170	EAL48611	Long chain fatty acid-CoA ligase (<i>Nostoc punctiforme</i>)	26	–	–	–	±
523.m00034	EAL43780	myb Family transcription factor (<i>Arabidopsis thaliana</i>)	28	–	–	±	±
49.m00176	EAL49211	NFI1 (<i>Saccharomyces cerevisiae</i>)	25	±	–	–	–
10.m00387	EAL51182	Oxysterol-binding protein 1 (<i>Mus musculus</i>)	31	–	–	–	±
89.m00119	EAL47858	PRP8 protein ^a (<i>Oryza sativa</i>)	63	–	–	±	–
85.m00147	EAL47966	Rad54b ^a (<i>Gallus gallus</i>)	37	–	–	±	–
266.m00064	EAL44459	RNA polymerase ^a (<i>Pleurotus ostreatus</i>)	25	–	–	±	–
221.m00094	EAL45026	RNA processing factor 1 (<i>Homo sapiens</i>)	36	–	±	–	–
186.m00119	EAL45642	Tegument protein (<i>Human herpesvirus 6</i>)	26	–	+	–	–
198.m00102	EAL45413	Transcription factor 3B (<i>Dictyostelium discoideum</i>)	35	±	±	±	+
403.m00048	EAL43331	Translation elongation factor 1 α 1 (<i>Homo sapiens</i>)	75	+	+	+	+

Proteins absent in HM1 at all time points and present in KU33 or HATAJI at 0 or 30 min are shown. Proteins with the peptide coverage of >5%, 0.1–5%, or undetected at each time points are marked with “+”, “±”, “–”, respectively.

^a It indicates annotation used in the NCBI non-redundant database, while the protein is annotated differently in the *E. histolytica* Genome Database at TIGR.

(37%) represent strain-specific phagosome proteins. These data suggest that significant inter-strain variations of phagosome proteins and their kinetics exist. However, we may still overestimate the number of strain-specific proteins since the profiles of only two time points were compared among strains. One may argue that observed strain variations may be attributable to genetic polymorphism among isolates. However, this is not likely the case. First, the degree of the diversity at the protein level is small; for instance, a representative glycolytic enzyme glucose 6-phosphate isomerase revealed heterogeneous residues at only 2 positions among 546 amino acids (0.4%) among representative 4 isolates showing distinct zymodemes (Razmjou et al., unpublished). Second, we observed only a very limited number of peptides derived from the two clinical isolates showing low cross-correlation scores against the protein database of the reference HM1 strain. We detected only 0.2% mis- or poorly matched peptides (12 of 5583) obtained from phagosomes of the two clinical isolates. Therefore, the observed strain variations were not likely affected by the genetic polymorphisms among three strains.

Numerous cytoskeletal proteins, such as actin, actin-related protein, coronin 7, F-actin capping protein, formin, and villidin were detected only in HATAJI. Seven out of 10 cytoskeletal proteins detected in HM1 (Table 1) were also detected in HATAJI. These data suggest that cytoskeletal proteins are more abundant in phagosomes of HATAJI than those of HM1 and KU33. This result is consistent with our preliminary data that the internalization efficiency of yeasts, red blood cells, or beads is 4–14-fold higher in HATAJI than in HM1 and KU33 as measured with the number of particles ingested for 10–30 min (Mitra et al., unpublished). In addition, these strains were also significantly different in phagosomal pH and kinetics of degradation within phagosomes (Mitra et al., unpublished). These differences may be partially attributable to the variation of phagosome proteins among strains. One should be aware that KU33 and HATAJI were cultivated under different culture conditions (co-cultivated with *C. fasciculata*). To examine effects of co-cultivation with *C. fasciculata* on phagosome profiles, we compared the phagosome protein profiles at chase 0 min between HM1 cultivated in the axenic culture and HM1 cultivated with *C. fasciculata*. Among 103 proteins detected in phagosomes of axenically cultivated HM1, 95 proteins (92%) were also detected in phagosomes of monoxenically cultured HM1. This result clearly indicates that co-cultivation with *C. fasciculata* does not drastically affect a profile of phagosome proteins, and that the observed inter-strain variations are not attributable to different culture conditions.

In summary, we showed that the phagosome compositions dynamically and continuously change during phagosome maturation and the phagosome protein profiles are diverse among heterogeneous *E. histolytica* strains. Our proteomic data on kinetics and strain variation of phagosome biogenesis should give a basis of our knowledge of phagosome biogenesis, lead to further understanding of the functions of phagocytosis in this parasite, and also facilitate functional assignment of individual hypothetical proteins localized to phagosomes, which is essential for annotation of the genome database.

Acknowledgements

We are grateful to Nicholas Sherman, W.M. Keck Biomedical Mass Spectrometry Laboratory at the University of Virginia for technical support on MS analyses, Hiroshi Tachibana, Tokai University for Igl antibody, Sharon L. Reed, Departments of Pathology and Medicine at the University of California for CP1 antibody, Yumiko Saito-Nakano, Kumiko Nakada-Tsukui, Dan Sato, Bithwa N. Mitra, and Vahab AH, NIID for helpful discussions. The *E. histolytica* genome databases available at TIGR and Sanger, which were supported by grants from National Institute of Allergy and Infectious Diseases and Wellcome Trust, were utilized for MS analysis. This work was supported by a grant for Precursory Research for Embryonic Science and Technology, Japan Science and Technology Agency to T.N., Grant-in-Aid for Scientific Research on Priority Areas from the Ministry of Education, Culture, Sports, Science and Technology of Japan to T.N. (16017307, 16044250, 17390124), a grant from the Japan Health Sciences Foundation to T.N., a grant for research on emerging and re-emerging infectious diseases from the Ministry of Health, Labour and Welfare of Japan to T.N. and B.J.M., NIHA1053678 to C.D.H., NIHA132615 to B.J.M., and NIH AI26649 to W.A.P.

Appendix A. Supplementary data

Supplementary data associated with this article can be found, in the online version, at [10.1016/j.molbiopara.2005.10.001](https://doi.org/10.1016/j.molbiopara.2005.10.001).

References

- [1] World Health Organization. The world health report 1998: life in the 21st century—a vision for all. Geneva: World Health Organization Press; 1998.
- [2] Lima AA. Tropical diarrhoea: new developments in traveller's diarrhoea. *Curr Opin Infect Dis* 2001;14:547–52.
- [3] Westphal A, Michel R. Phagocytosis and pinocytosis of *Entamoeba histolytica*. *Z Tropenmed Parasitol* 1971;22:82–91.
- [4] Bracha R, Kobiler D, Mirelman D. Attachment and ingestion of bacteria by trophozoites of *Entamoeba histolytica*. *Infect Immun* 1982;36:396–406.
- [5] Tsutsumi V, Ramirez-Rosales A, Lanz-Mendoza H, et al. *Entamoeba histolytica*: erythrophagocytosis, collagenolysis, and liver abscess production as virulence markers. *Trans R Soc Trop Med Hyg* 1992;86:170–2.
- [6] Guerrant RL, Brush J, Ravdin JJ, Sullivan JA, Mandell GL. Interaction between *Entamoeba histolytica* and human polymorphonuclear neutrophils. *J Infect Dis* 1981;143:83–93.
- [7] Bracha R, Mirelman D. Virulence of *Entamoeba histolytica* trophozoites: effects of bacteria, microaerobic conditions, and metronidazole. *J Exp Med* 1984;160:353–68.
- [8] Sahoo N, Labruyere E, Bhattacharya S, Sen P, Guillen N, Bhattacharya A. Calcium binding protein 1 of the protozoan parasite *Entamoeba histolytica* interacts with actin and is involved in cytoskeleton dynamics. *J Cell Sci* 2004;117:3625–34.
- [9] Orozco E, Guarneros G, Martinez-Palomo A, Sanchez T. *Entamoeba histolytica*: phagocytosis as a virulence factor. *J Exp Med* 1983;158:1511–21.
- [10] Okada M, Huston CD, Mann BJ, Petri Jr WA, Kita K, Nozaki T. Proteomic analysis of phagocytosis in the enteric protozoan parasite *Entamoeba histolytica*. *Eukaryot Cell* 2005;4:827–31.
- [11] Haghghi A, Kobayashi S, Takeuchi T, Thammapalerd N, Nozaki T. Geographic diversity among genotypes of *Entamoeba histolytica* field isolates. *J Clin Microbiol* 2003;41:3748–56.

- [12] Diamond LS, Harlow DR, Cunnick CC. A new medium for the axenic cultivation of *Entamoeba histolytica* and other *Entamoeba*. *Trans R Soc Trop Med Hyg* 1978;72:431–2.
- [13] Clark CG, Diamond LS. Methods for cultivation of parasitic protists of clinical importance. *Clin Microbiol Rev* 2002;15:329–41.
- [14] Mann BJ, Chung CY, Dodson JM, Ashley LS, Braga LL, Snodgrass TL. Neutralizing monoclonal antibody epitopes of the *Entamoeba histolytica* galactose adhesin map to the cysteine-rich extracellular domain of the 170-kilodalton subunit. *Infect Immun* 1993;61:1772–8.
- [15] Cheng XJ, Hughes MA, Huston CD, et al. Intermediate subunit of the Gal/GalNAc lectin of *Entamoeba histolytica* is a member of a gene family containing multiple CXXC sequence motifs. *Infect Immun* 2001;69:5892–8.
- [16] McCoy JJ, Weaver AM, Petri Jr WA. Use of monoclonal anti-light subunit antibodies to study the structure and function of the *Entamoeba histolytica* Gal/GalNAc adherence lectin. *Glycoconj J* 1994;11:432–6.
- [17] Nozaki T, Asai T, Kobayashi S, et al. Molecular cloning and characterization of the genes encoding two isoforms of cysteine synthase in the enteric protozoan parasite *Entamoeba histolytica*. *Mol Biochem Parasitol* 1998;97:33–44.
- [18] Tokoro M, Asai T, Kobayashi S, Takeuchi T, Nozaki T. Identification and characterization of two isoenzymes of methionine gamma-lyase from *Entamoeba histolytica*: a key enzyme of sulfur-amino acid degradation in an anaerobic parasitic protist that lacks forward and reverse trans-sulfuration pathways. *J Biol Chem* 2003;278:42717–27.
- [19] Ali V, Shigeta Y, Tokumoto U, Takahashi Y, Nozaki T. An intestinal parasitic protist, *Entamoeba histolytica*, possesses a non-redundant nitrogen fixation-like system for iron-sulfur cluster assembly under anaerobic conditions. *J Biol Chem* 2004;279:16863–74.
- [20] Sanuki J, Nakano K, Tokoro M, et al. Purification and identification of major soluble 40-kDa antigenic protein from *Entamoeba histolytica*: its application for serodiagnosis of asymptomatic amebiasis. *Parasitol Int* 2001;50:73–80.
- [21] Loftus B, Anderson I, Davies R, et al. The genome of the protist parasite *Entamoeba histolytica*. *Nature* 2005;433:865–8.
- [22] Eng JK, McCormack AL, Yates JR. An approach to correlate tandem mass spectral data of peptides with amino acid sequence in a protein database. *J Am Soc Mass Spectrom* 1994;5:976–89.
- [23] Sambrook J, Fritsh EF, Maniatis T. *Molecular cloning: a laboratory manual*. 3rd ed. Cold Spring Harbor: Cold Spring Harbor Laboratory Press; 2001.
- [24] Saito-Nakano Y, Yasuda T, Nakada-Tsukui K, Leippe M, Nozaki T. Rab5-associated vacuoles play a unique role in phagocytosis of the enteric protozoan parasite *Entamoeba histolytica*. *J Biol Chem* 2004;279:49497–507.
- [25] Saito-Nakano Y, Loftus BJ, Hall N, Nozaki T. The diversity of Rab GTPases in *Entamoeba histolytica*. *Exp Parasitol* 2005;110:244–52.
- [26] Nakada-Tsukui K, Saito-Nakano Y, Ali V, Nozaki T. A retromer-like complex is a novel Rab7 effector that is involved in the transport of the virulence factor cysteine protease in the enteric protozoan parasite *Entamoeba histolytica*. *Mol Biol Cell*, in press.
- [27] Mitra BN, Kobayashi S, Saito-Nakano Y, Nozaki T. Differences in morphology of phagosomes and kinetics of acidification and degradation in phagosomes between the pathogenic *Entamoeba histolytica* and the non-pathogenic *Entamoeba dispar*. *Cell Motil Cytoskeleton* 2005;62:84–99.
- [28] Jensen MS, Bainton DF. Temporal changes in pH within the phagocytic vacuole of the polymorphonuclear neutrophilic leukocyte. *J Cell Biol* 1973;56:379–88.
- [29] Geisow MJ, D'Arcy Hart P, Young MR. Temporal changes of lysosome and phagosome pH during phagolysosome formation in macrophages: studies by fluorescence spectroscopy. *J Cell Biol* 1981;89:645–52.
- [30] Rupper A, Cardelli J. Regulation of phagocytosis and endo-phagosomal trafficking pathways in *Dictyostelium discoideum*. *Biochim Biophys Acta* 2001;1525:205–16.
- [31] Chua J, Deretic V. *Mycobacterium tuberculosis* reprograms waves of phosphatidylinositol 3-phosphate on phagosomal organelles. *J Biol Chem* 2004;279:36982–92.
- [32] Yam PT, Theriot JA. Repeated cycles of rapid actin assembly and disassembly on epithelial cell phagosomes. *Mol Biol Cell* 2004;15:5647–58.
- [33] Mann BJ. Structure and function of the *Entamoeba histolytica* Gal/GalNAc lectin. *Int Rev Cytol* 2002;216:59–80.
- [34] Gotthardt D, Warnatz HJ, Henschel O, Bruckert F, Schleicher M, Soldati T. High-resolution dissection of phagosome maturation reveals distinct membrane trafficking phases. *Mol Biol Cell* 2002;13:3508–20.
- [35] Pitt A, Mayorga LS, Stahl PD, Schwartz AL. Alterations in the protein composition of maturing phagosomes. *J Clin Invest* 1992;90:1978–83.
- [36] Simms HH, D'Amico R, Monfils P, Burchard KW. Altered polymorphonuclear leukocyte Fc gamma R expression contributes to decreased candidal activity during intraabdominal sepsis. *J Lab Clin Med* 1991;117:241–9.
- [37] Clark CG, Roger AJ. Direct evidence for secondary loss of mitochondria in *Entamoeba histolytica*. *Proc Natl Acad Sci USA* 1995;92:6518–21.
- [38] Beck DL, Boettner DR, Dragulev B, Ready K, Nozaki T, Petri Jr WA. Identification and gene expression analysis of a large family of transmembrane kinases related to the Gal/GalNAc lectin in *Entamoeba histolytica*. *Eukaryot Cell* 2005;4:722–32.
- [39] Haghghi A, Kobayashi S, Takeuchi T, Masuda G, Nozaki T. Remarkable genetic polymorphism among *Entamoeba histolytica* isolates from a limited geographic area. *J Clin Microbiol* 2002;40:4081–90.

Chemotherapeutic efficacy of ascofuranone in *Trypanosoma vivax*-infected mice without glycerol

Yoshisada Yabu^{a,*}, Takashi Suzuki^a, Coh-ichi Nihei^{b,1}, Nobuko Minagawa^c,
Tomoyoshi Hosokawa^d, Kazuo Nagai^e, Kiyoshi Kita^b, Nobuo Ohta^a

^a Department of Molecular Parasitology, Nagoya City University, Graduate School of Medical Sciences, Nagoya 467-8601, Japan

^b Department of Biomedical Chemistry, Graduate School of Medicine, The University of Tokyo, Tokyo 113-0033, Japan

^c Department of Biochemistry, Niigata College of Pharmacy, Niigata 950-2076, Japan

^d Institute of Applied Biology, Yokohama 222-0011, Japan

^e Department of Applied Biological Chemistry, Chubu University, Kasugai 487-8501, Japan

Received 8 August 2005; accepted 9 September 2005

Available online 9 November 2005

Abstract

Ascofuranone, an antibiotic isolated from *Ascochyta visiae*, showed trypanocidal activity in *Trypanosoma vivax*-infected mice. A single dose of 50 mg/kg ascofuranone effectively cured the mice without the help of glycerol. Repeated administrations of this drug further enhanced its chemotherapeutic effect. After two, three, and four consecutive days treatment, the doses needed to cure the infection decreased to 25, 12, and 6 mg/kg, so that the total doses administered were 50, 36 and 24 mg/kg, respectively. Ascofuranone (50 mg/kg) also had a prophylactic effect against *T. vivax* infection within the first two days after administration. This prophylactic activity diminished to 80% by day 3 and completely disappeared four days after administration. Of particular interest in this study was that ascofuranone had trypanocidal activity in *T. vivax*-infected mice in the absence of glycerol, whereas co-administration of glycerol or repeated administrations of this drug are needed for *Trypanosoma brucei brucei* infection. Our present results strongly suggest that ascofuranone is also an effective tool in chemotherapy against African trypanosomiasis in domestic animals. © 2005 Elsevier Ireland Ltd. All rights reserved.

Keywords: *Trypanosoma vivax*; Chemotherapy; Ascofuranone; Mouse; Intramuscular

1. Introduction

Trypanosoma vivax is a causative agent of trypanosomiasis in livestock, and, even in the absence of tsetse fly, various blood-sucking insects can transmit mechanically [1]. This parasitic disease is spreading in the large area of sub-Saharan Africa and the 13 South American countries [2]. In Africa, the most commonly employed drugs for treating trypanosomiasis in cattle, sheep, and goats are currently homidium, isometami-

dium, and diminazene [3]. These drugs were discovered more than forty years ago and their use has been challenged by the appearance of drug-resistant trypanosomes [4–8]. New drugs that are nontoxic to the host and more effective and specific against African trypanosome infection in domestic animals are eagerly awaited [3,6,9,10].

The antibiotic ascofuranone (Fig. 1), which was isolated from the phytopathogenic fungus *Ascochyta visiae*, was discovered as an anti-tumor drug that is dependent on the activation of host macrophages [11–18]. In a previous report [19], we showed that ascofuranone strongly inhibits both mitochondrial O₂ consumption in a mitochondrial preparation and the in vitro growth of the bloodstream form of *T. b. brucei*. Moreover, we have shown that ascofuranone specifically inhibits the alternative oxidase (AOX or TAO) of the respiratory chain of the long slender (LS) forms of *T. b. brucei* [19–25], whereas glycerol inhibits the remaining anaerobic ATP production by mass action [19,20,23,27–31]. In the combination treatment with ascofuranone and glycerol,

Abbreviations: AOX, alternative oxidase; TAO, trypanosome alternative oxidase; LS, long slender; SHAM, salicylhydroxamic acid; TbAOX, *T. b. brucei* AOX; rTbAOX, recombinant TbAOX; TvAOX, *T. vivax* AOX; rTvAOX, recombinant TvAOX; PBS, phosphate buffered saline; GK, glycerol kinase; G-3-P, L-glycerol-3-phosphate.

* Corresponding author. Tel.: +81 52 8538186; fax: +81 52 8420149.

E-mail address: yabu@med.nagoya-cu.ac.jp (Y. Yabu).

¹ Present address: Molecular Membrane Biology Laboratory, RIKEN, 2-1 Hirosawa, Wako 351-0198, Japan.

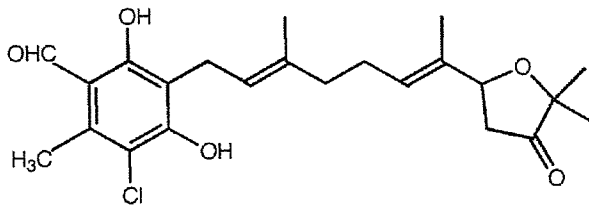


Fig. 1. Structure of ascofuranone.

trypanosomes were dramatically cleared from the infected mice. In fact, all bloodstream forms disappeared within 30 min of intraperitoneal treatment and within 180 min after oral administration [20]. Further, repeated administrations of ascofuranone also showed an anti-trypanosomal effect in the absence of glycerol against infection of *T. b. brucei* in mice [25]. These findings show that the mitochondrial respiratory chain of the African trypanosome is an attractive target for chemotherapy.

In an early study, Vickerman and Evans [32] showed that respiration of *T. vivax* was completely inhibited by 0.1 to 0.2 mM salicylhydroxamic acid (SHAM), an inhibitor of AOX. A combination of SHAM and glycerol was confirmed to have trypanocidal activity in *T. vivax*-infected mice [33,34], rats [29], and goats [35]. In a recent investigation, we cloned the *T. vivax* alternative oxidase (TvAOX) gene and characterized the recombinant enzyme [26]. We found that ascofuranone, the most potent known inhibitor of *T. b. brucei* AOX (TbAOX) [19], was also a competitive inhibitor of recombinant TvAOX (rTvAOX) with K_i value significantly lower than that of recombinant TbAOX (rTbAOX). Because of these findings and the current studies, we explored the chemotherapeutic efficacy of ascofuranone against *T. vivax* infection in mice.

2. Materials and methods

2.1. Chemicals

Ascofuranone [36] isolated from the fungus *Ascochyta visiae* was suspended in phosphate buffered saline (pH 7.5) containing 0.05% (v/v) Tween-20 (Wako Pure Chemical Co., Osaka, Japan) using a Teflon-glass homogenizer.

2.2. Trypanosomes

Trypanosoma vivax ILD at 1.2 [37] is a clone derived from of *T. vivax* Y486, isolated from an infected Zebu cow in Zaria, Nigeria and which is a naturally rodent-infective stock [38]. This clone was kindly provided by Dr. P.R. Gardiner, International Laboratory for Research on Animal Diseases (ILRAD), Nairobi, Kenya [39]. The clone maintained in Balb/c mice (Japan SLC Co., Hamamatsu, Shizuoka, Japan) weighing 18 to 20 g by serial transfer at 6 day intervals was used throughout the experiment.

2.3. Animals

Balb/c mice (male, 6-week-old; Japan SLC Co.) were used for the current studies because they are susceptible to *T. vivax* infection [40].

2.4. Experimental treatments

Mice were inoculated intraperitoneally with 10^4 of bloodstream form of *T. vivax* from a previously infected mouse. After five days, ascofuranone was administered intramuscularly to trypanosome-infected mice every 24 h for one

to four consecutive days. Four groups of five mice received daily intramuscular administration of ascofuranone (50, 25, 12, or 6 mg/kg) for one to four consecutive days. Control mice received only PBS containing 0.05% (v/v) Tween-20. After treatment, parasitemia was checked every day by observing tail blood smears. Mice that were negative for trypanosomes for 60 days after the last treatment were considered cured [41]. The animal research committee of Nagoya City University, Graduate School of Medical Sciences, approved this study.

3. Results

Experiments were started 5 days after infection of *T. vivax*. At the start of treatment, parasitemia level in infected mice was over 10^5 trypanosomes/ml. Without treatment, all mice died within 10 days after infection. In the present study, we adopted intramuscular administration of ascofuranone because intravenous and intramuscular injection is common in the treatment of infected domestic animals in the field. The chemotherapeutic efficacy of ascofuranone against *T. vivax* infection is summarized in Table 1. A single treatment with 50 mg/kg ascofuranone effectively cured all mice without the aid of glycerol. At a dose of 25 mg/kg ascofuranone, two consecutive days administration were needed for recovery from the infection. In mice treated once with 25 mg/kg ascofuranone, four out of five were cured, but bloodstream forms reappeared in the remaining mouse after 11 days, and it died 17 days after the treatment. In mice treated with 12 mg/kg ascofuranone, three consecutive days administration was required to permanently cure them from the infection (total dose: 36 mg/kg). In mice treated once with 12 mg/kg, one out of five mice was cured, but trypanosomes reappeared in four mice 6 to 8 days, and they died 12 to 14 days after the beginning of treatment. In mice treated twice with this dose of ascofuranone, two out of five were cured, but trypanosomes reappeared in three 8 to 11 days, and they died 14 to 17 days after the initiation of the treatment. When infected mice were treated with 6 mg/kg ascofuranone, four consecutive days administration was needed for the clearance of the infection (total dose: 24 mg/kg). When 6 mg/kg ascofuranone was administered for one or two consec-

Table 1
Effects of ascofuranone on *Trypanosoma vivax* infection in mice

Ascofuranone ^a (mg/kg)	Days of consecutive administration	Days of parasitemia reappearance and death occurred after beginning of treatment		Cure rate ^c (%)
		Parasitemia	Death	
PBS	5	N ^b	5	0
6	1	N ^b	6–7	0
	2	1–2	7–8	0
	3	7–9	13–15	40
	4	–	Cured	100
12	1	6–8	12–14	20
	2	8–11	14–17	40
	3	–	Cured	100
25	1	11	17	80
	2	–	Cured	100
50	1	–	Cured	100

^a Ascofuranone was administered intramuscularly.

^b Parasites did not disappear.

^c Each group consists of five mice.

utive days, all infected mice died, and there was only a prolongation of the survival time. In mice treated for three consecutive days with 6 mg/kg ascofuranone, two out of five mice were cured, whereas the remaining mice relapsed 7 to 9 days, and they died 13 to 15 days after the beginning of treatment. Trypanosomes in the mice treated with 12 to 50 mg/kg ascofuranone disappeared from the blood within 12 h after the first administration. However, in infected mice receiving only a single administration of 6 mg/kg ascofuranone, trypanosomes did not disappear from the blood, and there was only a prolongation of the survival time. On the other hand, in infected mice administered 6 mg/kg ascofuranone for two to four consecutive days, there was a disappearance of trypanosomes from the blood within 24 to 48 h. Finally, the 50% lethal dose (LD₅₀) of ascofuranone administered intramuscularly for 4 consecutive days was estimated to be 800 mg/kg/day.

We next examined the prophylactic activity of ascofuranone. Groups of five mice each were injected intraperitoneally with 10⁴ trypanosomes one to five days after administration of 50 mg/kg ascofuranone. As shown in Table 2, complete protection against *T. vivax* infection continued for two days, but this activity decreased to 80% by day three, and there was no effect observed 4 days after administration.

4. Discussion

Our present studies clearly demonstrate that ascofuranone acts as a trypanocidal drug in *T. vivax*-infected mice. In the preliminary experiments, we also confirmed trypanocidal effect of ascofuranone combination with glycerol in *T. vivax* infected mice (data not shown). However, we only determined the anti-trypanosomal activity of ascofuranone in a single or consecutive treatment without glycerol, because simple mode of administration is a very important factor in rural conditions. Fortunately, there was no requirement for glycerol as there is in mice infected with *T. b. brucei* [19,20], which is the causative agent of African sleeping sickness. All *T. vivax*-infected mice receiving a single 50 mg/kg dose of ascofuranone were effectively cured.

The idea that African trypanosomiasis might be cured with a combination of ascofuranone and glycerol is based on the effects of these chemicals on the unique energy-metabolizing

pathway of the mammalian-infecting long slender (LS) bloodstream forms of this parasite. Energy production in the LS (host-infecting) forms of African trypanosomes is dependent on glycolysis within the glycosome, a peroxisome-like organelle specific to the parasite [30,42–44]. The mitochondrial cyanide-insensitive G-3-P oxidase system is used to re-oxidize NADH produced in the glycolytic pathway. This system oxidizes G-3-P produced in the glycosome using an electron transport system in the inner mitochondrial membrane that consists of G-3-P dehydrogenase, ubiquinone, and alternative oxidase (AOX) [19–29,42,45–58]. Under anaerobic conditions or in the presence of a respiratory inhibitor such as SHAM, G-3-P accumulates inside the glycosome and is converted to glycerol by the reverse reaction of glycerol kinase (GK) [30,31,42–44,59]. In this anaerobic glycolytic pathway, glucose is degraded to same amounts of pyruvate and glycerol, with a net synthesis of 1 mol of ATP per molecule of glucose degraded, even under anaerobic conditions or in the presence of inhibitors [30,31,42–44,59]. Therefore, inhibition of cyanide-insensitive respiration alone is not sufficient to kill the trypanosome, and the parasite can survive as long as glycerol does not accumulate in the medium. As we described previously [19], ascofuranone inhibited the electron-transport system of the LS forms of *T. b. brucei*, especially a mitochondrial enzyme TbAOX.

In the presence of ascofuranone, G-3-P cannot be re-oxidized, and G-3-P accumulates inside the glycosome and is converted to glycerol by the reverse reaction of glycerol kinase (GK). This alternative glycolytic pathway is inhibited by glycerol via mass action [19,20,23,27–31]. This combination treatment of ascofuranone and glycerol showed dramatic clearance of *T. b. brucei* infection in mice within 30 min after intraperitoneal administration [20]. Kralova et al. [59] have investigated the differences in the properties of GKs within the subgenus *Trypanozoon* (*T. b. brucei*, *T. b. gambiense*, *T. b. rhodesiense*, *T. evansi*, and *T. equiperdum*) and other Trypanosomatidae. The activity of GK for glycerol and G-3-P could be attributed to the Ala at position 137. An alanine occurs in GK of the subgenus *Trypanozoon*, and it has the ability to produce large amounts of glycerol, whereas GK of *T. vivax* and *T. congolense* contains a serine and has little or no capacity to produce glycerol. The present results clearly demonstrate the property of *T. vivax* GK that G-3-P accumulated in the glycosome is not converted rapidly following administration of ascofuranone and it might cause the death of trypanosomes in the absence of glycerol.

In the recent study we cloned the TvAOX gene and expressed the recombinant enzyme in *E. coli* [26]. Ascofuranone, which is the most potent inhibitor of rTbAOX, inhibited rTvAOX at low concentration. Recombinant TvAOX was more sensitive to ascofuranone than rTbAOX. This higher sensitivity of rTvAOX was consistent with the efficacy of ascofuranone in *T. vivax*-infected mice: administration of 100 mg/kg ascofuranone for four consecutive days is needed to cure mice infected with *T. b. brucei* [25], whereas the *T. vivax*-infected mice were cured with four treatments of only 6 mg/kg ascofuranone.

Table 2
Prophylactic effect of ascofuranone against infection of *Trypanosoma vivax* in mice^a

Days after administration ^b	No. of mice		Protection ^c rate (%)
	Protected	Dead	
1	5	0	100
2	5	0	100
3	4	1	80
4	0	5	0
5	0	5	0

^a *T. vivax* (10⁴) was inoculated intraperitoneally one to five days after administration of 50 mg/kg ascofuranone.

^b Ascofuranone was administered intramuscularly.

^c Each group consists of five mice.

Our experiment showed that ascofuranone had a 100% to 80% prophylactic activity for three days after administration. Further immunological, biochemical, and cell biological investigations are necessary to understand this interesting phenomenon.

Our results strongly suggest that ascofuranone is a promising candidate as a chemotherapeutic agent to treat African trypanosomiasis in domestic animals. We therefore have an ongoing project in Africa to evaluate the efficacy of ascofuranone in *T. vivax*-infected livestock.

Acknowledgments

This work was supported by a grant for Research on Emerging and Reemerging Infectious Diseases, and a grant for International Health Cooperation Research (15-C5) from the Ministry of Health, Labor, and Welfare of Japan as well as by a Grant-in-Aid for Scientific Research on Priority Areas from the Ministry of Education, Science, Culture and Sport of Japan (13226015 and 13854011). This study was also supported by the Pilot Applied Research Project for the Industrial Use of Space of the National Space Development Agency of Japan (NASDA) and the Japan Space Utilization Promotion Center (JSUP).

References

- [1] Gardiner PR. Recent studies of the biology of *Trypanosoma vivax*. *Adv Parasitol* 1989;28:229–317.
- [2] Jones TW, Davila AM. *Trypanosoma vivax*—out of Africa. *Trends Parasitol* 2001;17:99–101.
- [3] Wang CC. Molecular mechanisms and therapeutic approaches to the treatment of African trypanosomiasis. *Annu Rev Pharmacol Toxicol* 1995;35:93–127.
- [4] Schonefeld A, Rottcher D, Moloo SK. The sensitivity to trypanocidal drugs of *Trypanosoma vivax* isolated in Kenya and Somalia. *Trop Med Parasitol* 1987;38:177–80.
- [5] Codjia V, Mulatu W, Majiwa PA, Leak SG, Rowlands GJ, Authie E, et al. Epidemiology of bovine trypanosomiasis in the Ghibe valley, southwest Ethiopia. 3. Occurrence of populations of *Trypanosoma congolense* resistant to diminazene, isometamidium and homidium. *Acta Trop* 1993;53:151–63.
- [6] Geerts S, Holmes PH, Eisler MC, Diall O. African bovine trypanosomiasis: the problem of drug resistance. *Trends Parasitol* 2001;17:25–8.
- [7] Ainanshe OA, Jennings FW, Holmes PH. Isolation of drug-resistant strains of *Trypanosoma congolense* from the lower Shabelle region of Southern Somalia. *Trop Anim Health Prod* 1992;24:65–73.
- [8] Sinyangwe L, Delespaux V, Brandt J, Geerts S, Mubanga J, Machila N, et al. Trypanocidal drug resistance in eastern province of Zambia. *Vet Parasitol* 2004;119:125–35.
- [9] Kuzoe FAS. Current situation of African trypanosomiasis. *Acta Trop* 1993;54:153–62.
- [10] Keiser J, Stich A, Burri C. New drugs for the treatment of human African trypanosomiasis: research and development. *Trends Parasitol* 2001;17:42–9.
- [11] Magae J, Hosokawa T, Ando K, Nagai K, Tamura G. Antitumor protective property of an isoprenoid antibiotic, ascofuranone. *J Antibiot* 1982;35:1547–52.
- [12] Magae J, Nagai K, Ando K, Yamasaki M, Tamura G. Effects of an antitumor agent, ascofuranone, on the macromolecular syntheses of intact cells. *J Antibiot* 1983;36:892–9.
- [13] Magae J, Hotta M, Nagai K, Suzuki S, Ando K, Yamasaki M, et al. Activation of natural cytotoxic activity and concomitant reduction of triglyceride content of murine spleen, treated with an antitumor antibiotic, ascofuranone. *J Antibiot* 1986;39:676–81.
- [14] Magae J, Suzuki S, Nagai K, Yamasaki M, Ando K, Tamura G. In vitro effects of an antitumor antibiotic, ascofuranone, on the murine immune system. *Cancer Res* 1986;46:1073–8.
- [15] Magae J, Nagai K, Suzuki S, Yamasaki M, Ando K, Tamura G. Macrophage-specific effect on lipid metabolism by an antibiotic, ascofuranone. *J Antibiot* 1987;40:202–8.
- [16] Magae J, Hosokawa T, Matsuda Y, Hotta M, Hayasaki J, Nagai K, et al. Suppression of hypertriglyceridemia of Ehrlich carcinoma-bearing mice by an antibiotic, ascofuranone. *Cancer Res* 1987;47:96–9.
- [17] Magae J, Hayasaki J, Matsuda Y, Hotta M, Hosokawa T, Suzuki S, et al. Antitumor and antimetastatic activity of an antibiotic, ascofuranone, and activation of phagocytes. *J Antibiot* 1988;41:959–65.
- [18] Magae J, Nagai K, Ando K, Tamura G. Differentiation of mouse and human myeloid leukemia cells induced by an antitumor antibiotic, ascofuranone. *Agric Biol Chem* 1988;52:3143–7.
- [19] Minagawa N, Yabu Y, Kita K, Nagai K, Ohta N, Meguro K, et al. An antibiotic, ascofuranone, specifically inhibits respiration and in vitro growth of long slender bloodstream forms of *Trypanosoma brucei*. *Mol Biochem Parasitol* 1996;81:127–36.
- [20] Yabu Y, Minagawa N, Kita K, Nagai K, Honma M, Sakajo S, et al. Oral and intraperitoneal treatment of *Trypanosoma brucei brucei* with a combination of ascofuranone and glycerol in mice. *Parasitol Int* 1998;47:131–7.
- [21] Fukai Y, Amino H, Hirawake H, Yabu Y, Ohta N, Minagawa N, et al. Functional expression of the ascofuranone-sensitive *Trypanosoma brucei brucei* alternative oxidase in the cytoplasmic membrane of *Escherichia coli*. *Comp Biochem Physiol C* 1999;124:141–8.
- [22] Fukai Y, Nihei C, Yabu Y, Suzuki T, Ohta N, Minagawa N, et al. Strain-specific difference in amino acid sequences of trypanosome alternative oxidase. *Parasitol Int* 2002;51:195–9.
- [23] Nihei C, Fukai Y, Kita K. Trypanosome alternative oxidase as a target of chemotherapy. *Biochim Biophys Acta* 2002;1587:234–9.
- [24] Nihei C, Fukai Y, Kawai K, Osanai A, Yabu Y, Suzuki T, et al. Purification of active recombinant trypanosome alternative oxidase. *FEBS Lett* 2003;538:35–40.
- [25] Yabu Y, Yoshida A, Suzuki T, Nihei C, Kawai K, Minagawa N, et al. The efficacy of ascofuranone in a consecutive treatment on *Trypanosoma brucei brucei* in mice. *Parasitol Int* 2003;52:155–64.
- [26] Suzuki T, Nihei C, Yabu Y, Hashimoto T, Suzuki M, Yoshida A, et al. Molecular cloning and characterization of *Trypanosoma vivax* alternative oxidase (AOX) gene, a target of the trypanocide ascofuranone. *Parasitol Int* 2004;53:235–45.
- [27] Clarkson Jr AB, Grady RW, Grossman SA, McCallum RJ, Brohn FH. *Trypanosoma brucei brucei*: a systematic screening for alternatives to the salicylhydroxamic acid–glycerol combination. *Mol Biochem Parasitol* 1981;3:271–91.
- [28] van der Meer C, Versluijs-Broers JA, Opperdoes FR. *Trypanosoma brucei*: trypanocidal effect of salicylhydroxamic acid plus glycerol in infected rats. *Exp Parasitol* 1979;48:126–34.
- [29] van der Meer C, Versluijs-Broers JA. *Trypanosoma brucei* and *T. vivax*: salicylhydroxamic acid and glycerol treatment of acute and chronically infected rats. *Exp Parasitol* 1986;62:98–113.
- [30] Clayton CE, Michels P. Metabolic compartmentation in African trypanosomes. *Parasitol Today* 1996;12:465–71.
- [31] Michels PAM, Hannaert V, Bringaud F. Metabolic aspects of glycosomes in Trypanosomatidae—new data and views. *Parasitol Today* 2000;16:482–9.
- [32] Vickerman K, Evans DA. Studies on the ultrastructure and respiratory physiology of *Trypanosoma vivax* trypomastigote stages. *Trans R Soc Trop Med Hyg* 1974;68:145.
- [33] Evans DA, Holland MF. Effective treatment of *Trypanosoma vivax* infections with salicylhydroxamic acid (SHAM). *Trans R Soc Trop Med Hyg* 1978;72:203–4.
- [34] Evans DA, Brightman CA. Pleomorphism and the problem of recrudescence parasitemia following treatment with salicylhydroxamic acid (SHAM) in African trypanosomiasis. *Trans R Soc Trop Med Hyg* 1980;74:601–4.

- [35] van der Meer C, Versluis-Broers JA, van Duin CT, van den Ingh TS, Nieuwenhuijs J, Zwart D. Pitfalls of salicylhydroxamic acid plus glycerol treatment of *T. vivax* infected goats. *Tropenmed Parasitol* 1980;31:275–82.
- [36] Sasaki H, Hosokawa T, Sawada M, Ando K. Isolation and structure of ascofuranone and ascofuranol, antibiotics with hypolipidemic activity. *J Antibiot* 1973;26:676–80.
- [37] Barry JD, Gathuo H. Antigenic variation in *Trypanosoma vivax*: isolation of a serodome. *Parasitol* 1984;89:49–58.
- [38] Leeftang P, Buys J, Blotkamp C. Studies on *Trypanosoma vivax*: infectivity and serial maintenance of natural bovine isolates in mice. *Int J Parasitol* 1976;6:413–7.
- [39] Vos GJ, Gardiner PR. Antigenic relatedness of stocks and clones of *Trypanosoma vivax* from East and West Africa. *Parasitol* 1900;100:101–6.
- [40] de Gee AL, Shah SD, Doyle JJ. *Trypanosoma vivax*: courses of infection with three stabilates in inbred mouse strains. *Exp Parasitol* 1982;54:33–9.
- [41] Zhang ZQ, Giroud C, Baltz T. In vivo and in vitro sensitivity of *Trypanosoma evansi* and *T. equiperdum* to diminazene, suramin, Melcy, quinapyramine and isometamidium. *Acta Trop* 1991;50:101–10.
- [42] Tielens AGM, Van Hellemond JJ. Difference in energy metabolism between Trypanosomatidae. *Parasitol Today* 1998;14:265–71.
- [43] Visser N, Opperdoes FR. Glycolysis of *Trypanosoma brucei*. *Eur J Biochem* 1980;103:623–32.
- [44] Hannaert V, Michels PAM. Structure, function, and biogenesis of glycosomes in Kinetoplastida. *J Bioenerg Biomembr* 1994;26:205–12.
- [45] Clarkson Jr AB, Brohn FH. Trypanosomiasis: an approach to chemotherapy by the inhibition of carbohydrate catabolism. *Science* 1976;194:204–6.
- [46] Opperdoes FR, Borst P, Bakker S, Leene W. Localization of glycerol-3-phosphate oxidase in the mitochondrion and particulate NAD⁺-linked glycerol-3-phosphate dehydrogenase in the microbodies of the bloodstream form to *Trypanosoma brucei*. *Eur J Biochem* 1977;76:29–39.
- [47] Grady RW, Bienen EJ, Clarkson Jr AB. Esters of 3,4-dihydroxybenzoic acid, highly effective inhibitors of the sn-glycerol-3-phosphate oxidase of *Trypanosoma brucei brucei*. *Mol Biochem Parasitol* 1986;21:55–63.
- [48] Grady RW, Bienen EJ, Clarkson Jr AB. *p*-Alkyloxybenzhydroxamic acids, effective inhibitors of the trypanosome glycerol-3-phosphate oxidase. *Mol Biochem Parasitol* 1986;19:231–40.
- [49] Clarkson Jr AB, Bienen EJ, Pollakis G, Grady RW. Trypanocidal CoQ analogues: their effect on other mitochondrial system. *Comp Biochem Physiol B* 1989;94:245–51.
- [50] Clarkson Jr AB, Bienen EJ, Pollakis G, Saric M, McIntosh L, Grady R.W. Trypanosome alternative oxidase. Chemotherapy for trypanosomiasis. Proceedings of a workshop held at ILRAD, Nairobi, Kenya; 1989. p. 43–8.
- [51] Clarkson Jr AB, Bienen EJ, Pollakis G, Grady RW. Respiration of bloodstream forms of the parasite *Trypanosoma brucei brucei* is dependent on a plant-like alternative oxidase. *J Biol Chem* 1989;264:17770–6.
- [52] Bienen EJ, Saric M, Pollakis G, Grady RW, Clarkson Jr AB. Mitochondrial development in *Trypanosoma brucei brucei* transitional bloodstream forms. *Mol Biochem Parasitol* 1991;45:185–92.
- [53] Komblatt JA, Nthale J, McOdimba F. Purification of sn-glycerol-3-phosphate dehydrogenase from *Trypanosoma brucei brucei*. *Biochem Cell Biol* 1992;70:136–41.
- [54] Grady R.W, Bienen EJ, Dieck HA, Saric M, Clarkson Jr AB. *N-n*-alkyl-3,4-dihydroxybenzamidates as inhibitors of the trypanosome alternative oxidase: activity in vitro and in vivo. *Antimicrob Agents Chemother* 1993;37:1082–5.
- [55] Priest JW, Hajduk SL. Developmental regulation of mitochondrial biogenesis in *Trypanosoma brucei*. *J Bioenerg Biomembr* 1994;26:179–91.
- [56] Chaudhuri M, Ajayi W, Temple S, Hill GC. Identification and partial purification of a stage-specific 33 kDa mitochondrial protein as the alternative oxidase of the *Trypanosoma brucei brucei* bloodstream trypomastigotes. *J Eukaryot Microbiol* 1995;42:467–72.
- [57] Chaudhuri M, Hill GC. Cloning, sequencing, and functional activity of the *Trypanosoma brucei brucei* alternative oxidase. *Mol Biochem Parasitol* 1996;83:125–9.
- [58] Opperdoes FR. Progress in human African trypanosomiasis, sleeping sickness. Paris: Springer; 1999. p. 53–80.
- [59] Kralova I, Rigden DJ, Opperdoes FR, Michels PA. Glycerol kinase of *Trypanosoma brucei*. Cloning, molecular characterization and mutagenesis. *Eur J Biochem* 2000;267:2323–33.

Early detection of *Schistosoma mansoni* infection by touchdown PCR in a mouse model

Tomoyuki Suzuki ^a, Yoshio Osada ^a, Takashi Kumagai ^a, Atsuo Hamada ^b,
Eiichi Okuzawa ^b, Tamotsu Kanazawa ^{a,*}

^a Department of Parasitology and Tropical Public Health, University of Occupational and Environmental Health, Japan 1-1 Iseigaoka, Yahatanishi-ku, Kitakyushu, 807-8555, Japan

^b Japan Overseas Health Administration Center, Yokohama, Japan

Received 22 February 2006; received in revised form 11 May 2006; accepted 17 May 2006

Available online 5 July 2006

Abstract

A detection assay for *Schistosoma mansoni* DNA in mouse serum samples based on touchdown PCR was developed and evaluated. The serum samples could be assayed directly without the need to extract DNA. No cross reactions between *S. mansoni* and related species inducing human schistosomiasis were observed. After the infection, mouse sera and feces were collected for 8 weeks. Anti-worm antigen IgG and anti-soluble egg antigen IgG were detected in the sera at 6 weeks post-infection by ELISA. The parasite's eggs were detected in the feces at 8 weeks. In contrast, *S. mansoni* DNA was detected in the sera at 2 weeks post-infection. These data suggest that touchdown PCR is a potential tool for the early diagnosis of *S. mansoni* infection.

© 2006 Elsevier Ireland Ltd. All rights reserved.

Keywords: Schistosomiasis; *Schistosoma mansoni*; PCR; Diagnosis

1. Introduction

Schistosomiasis is a major parasitic disease of widespread endemicity in the tropics and subtropics. The disease affects people living in 74 endemic countries and has significant public health consequences [1]. It is estimated that about 400 million people are exposed to risk of *Schistosoma mansoni* infection in sub-Saharan Africa [2]. Despite intensive control programs with the use of effective drugs, the disease has not yet become under control [3]. In non-endemic countries, the prevalence of imported schistosomiasis is rising, owing to an increase in travel to endemic areas [4,5]. A wide range of diagnostic techniques for acute, chronic, and past schistosomiasis, including various parasitological methods for detecting eggs in feces or urine and methods for detecting antibody and antigen, is in use both for routine diagnosis and for research purposes [6]. Each of these methods has its advantages and

disadvantages [7,8]. The development of novel diagnostic tools is awaited.

The polymerase chain reaction (PCR) has proven useful in the clinical testing of a wide variety of pathogenic infections, such as human immunodeficiency virus [9], *Legionella pneumophila* [10], *Mycobacterium tuberculosis* [11], *Plasmodium falciparum* [12], *Trypanosoma cruzi* [13], and *Leishmania braziliensis* [14]. Recently, PCR-based methods for detecting *S. mansoni* and *S. haematobium* DNA from clinical samples and the intermediate hosts were also developed [15–19]. Some of these reports [17,18] used the 121-bp highly repeated sequence unit of *S. mansoni* genomic DNA reported by Hamburger et al. [20] as a target sequence. This technique was applied for the detection of cercariae in water [17] or infected snails [18] and has real potential. Pontes et al. reported on the usefulness of PCR for detecting *S. mansoni* DNA in human feces and serum samples [21].

In this article, we report the potential of touchdown PCR for the diagnosis of *S. mansoni* infection, with special reference to how early the infection can be detected, compared with other methods, through experiments with animals.

* Corresponding author. Tel.: +81 93 691 7432; fax: +81 93 602 4488.

E-mail address: t-kana@med.uoeh-u.ac.jp (T. Kanazawa).

2. Materials and methods

2.1. Maintenance of schistosomes and recovery of adult worms and eggs

S. mansoni (Puerto Rican strain) and *Schistosoma japonicum* (Japanese Yamanashi strain) were maintained by using female ICR mice as final hosts (SLC, Japan). *S. haematobium* (Kenyan strain) was maintained by using female ICR mice or female hamsters. As intermediate host snails, *Biomphalaria glabrata* (Puerto Rican strain), *Oncomelania hupensis nosohora* (Japanese Yamanashi strain) and *Bulinus globosus* (Kenyan strain) were used for *S. mansoni*, *S. japonicum* and *S. haematobium*, respectively. Mice or hamsters were infected percutaneously under anesthesia with pentobarbital sodium. Each animal was infected with 300–500 cercariae of *S. haematobium*, 30–50 cercariae of *S. japonicum* or 200 cercariae of *S. mansoni*. Six to seven weeks (*S. japonicum* and *S. mansoni*) or 4 months (*S. haematobium*) after the infection, the portal system of the infected animals was perfused with physiological saline containing 0.45% trisodium citrate to collect adult worms. Thereafter, the livers of infected rodents, which contained the parasite's eggs, were minced and homogenized. The liver homogenate was then digested with 1.8% NaCl solution containing 0.5 mg/mL collagenase (Wako Pure Chemical Industries, Japan) and 1 mg/mL actinase E (Kaken Pharmaceutical, Japan) for 6 h at 37°C. Eggs were purified by repetitive centrifugation at 150×g for 5 min. The adult worms and eggs were washed with physiological saline and kept frozen at –80°C until DNA extraction and antigen preparation. All the animal experiments were performed under the control of the Ethics Committee of Animal Care and Experimentation in accordance with The Guiding of Principles for Animal Care Experimentation, University of Occupational and Environmental Health, Japan and the Japanese Law for Animal Welfare and Care (No. 221).

2.2. Preparation of SWAP and SEA

Soluble worm antigen preparation (SWAP) and soluble egg antigen (SEA) were prepared as described previously [22]. Briefly, the adult worms or the eggs were homogenized in PBS by ultrasonic treatment and the homogenates were centrifuged at 20,000×g for 20 min. Supernatants (designated as SWAP and SEA) were collected and kept frozen at –80°C until use.

2.3. Experimental infection of mice with *S. mansoni* and collection of samples

Female ICR mice (7 weeks old) were infected with 200 cercariae of *S. mansoni* through tail skin. Three days and 1–8 weeks post-infection, four mice each were randomly chosen from among the infected animals and blood was collected by cardiac puncture. Serum of each mouse was separated by centrifugation (1500×g for 15 min) and kept frozen at –80°C until use. Equal amounts of each serum collected at the same

time were pooled for some PCR experiments. Adult worms were harvested by portal perfusion after the bleeding to verify successful infection of the mice. The small intestines were washed with physiological saline and digested with 4% KOH. After the digestion, eggs in the undigested debris were counted to check the presence of deposited eggs in the digestive tract. Feces excreted during 24 h before sacrifice were collected for the examination of stools.

2.4. DNA extraction


Genomic DNA was isolated from adults of each schistosome species. The extraction was carried out with a standard DNA isolation kit, Sepa Gene® (Sanko-Jyunyaku, Tokyo, Japan). The DNA was dissolved in TE (10 mM Tris–HCl, 1 mM EDTA pH 8.0) and kept at –20°C until use. The concentration of DNA was determined with a Gene Quant (Amersham, NJ, USA) spectrophotometer.

2.5. Touchdown PCR

The 121-bp tandem repeat DNA sequence unit of *S. mansoni* described previously [20] was selected for our experiments. Primers for the touchdown PCR were 5'-CCGAC-CAACCGTTCTATGAA-3' and 5'-CCCACGCTCTCG-CAAATAAT-3'. The expected length of the product of the amplification was 92 bp. The genomic DNA extracted from adult worms was used as the template except in one experiment (Fig. 3), in which schistosome-infected mouse sera were used directly as templates without a DNA extraction step. Twenty microliters of reaction mixture contained the following: 2 µL of a template, 0.2 mM dNTP, 1 µM of each primer, 0.5 U of KOD-Dash *Taq* polymerase and 1×KOD-Dash buffer (TOYOBO, Osaka, Japan). Touchdown PCR was performed by using a GeneAmp PCR System 2700 (Applied Biosystems, CA, USA). The conditions for the PCR are summarized in Table 1. A two-step cycle was applied in the touchdown PCR; i.e. a denaturing step and an annealing step. The annealing temperature (60°C) was gradually lowered (2°C after each set of 3 cycles) to 50°C. A twenty-cycle amplification was then performed with an annealing temperature of 50°C. The PCR products were separated by electrophoresis in 2.5% agarose gel and subjected to ethidium bromide staining. By sequencing of the cloned amplification product, it was verified to be identical to the part of the 121-bp highly repeated DNA sequence (data not shown).

Table 1
Conditions for touchdown PCR

	95 °C					
	30s					
Annealing	60 °C 30s	58 °C 30s	56 °C 30s	54 °C 30s	52 °C 30s	50 °C 30s
Cycle	3	3	3	3	3	20



2.6. Microplate-ELISA

Microplate-ELISA was performed as described previously with slight modifications [23]. SWAP or SEA was diluted with 25 mM bicarbonate buffer (pH 9.6) to 5 µg/mL and added to the wells of 96-well microplates. The plates were kept at 4°C overnight for antigen coating. After the removal of unbound antigens from the wells with washing buffer (PBS containing 0.05% Tween 20), 200 µL of blocking/dilution buffer (washing buffer containing 1% bovine serum albumin and 0.05% NaN₃) was added and the microplates were kept at room temperature for 2 h. Serum samples from infected mice diluted 1:100 were added to the wells. The plates were incubated at room temperature for 1 h. After three washes of the wells, 1:1000 dilution of anti-mouse IgG (γ-specific) labeled with peroxidase (Sigma, St. Louis, MO) was added and the plates were incubated at room temperature for 30 min. ABTS (2,2' azino-bis(3-ethyl-benzthiazoline-6-sulphonic acid) substrate solution (Moss Inc., Pasadena, MD) was used for coloring. The optical density of each well was measured at 415 nm.

2.7. Stool examination

Eggs in the stools were counted according to a previously described method [24] with slight modifications. Briefly, approximately 500 mg of each stool sample was suspended in 10 mL of 10% formalin solution. Then, all the eggs in 400 µL of the suspension were counted microscopically. The number of eggs per gram (EPG) of feces was calculated.

3. Results

3.1. Sensitivity and species-specificity of the touchdown PCR

To determine the detectable level of *S. mansoni* DNA, a series of diluted samples of genomic DNA were amplified by the touchdown PCR. The expected product was observed

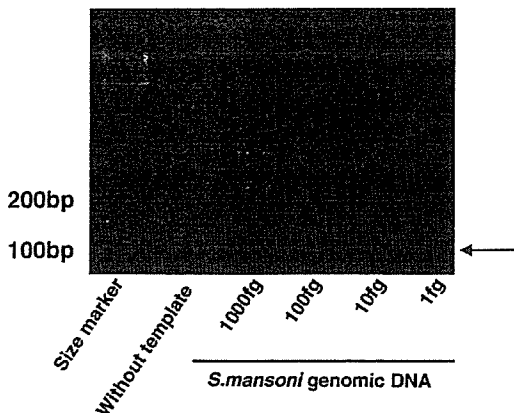


Fig. 1. Sensitivity of the touchdown PCR. One picogram, 100 fg, 10 fg or 1 fg of genomic DNA from *S. mansoni* was amplified by the touchdown PCR. The size of the appropriate PCR products is indicated by an arrow on the right. The lengths of the size marker are indicated in b.p. on the left. Data representative of repeated experiments is shown.

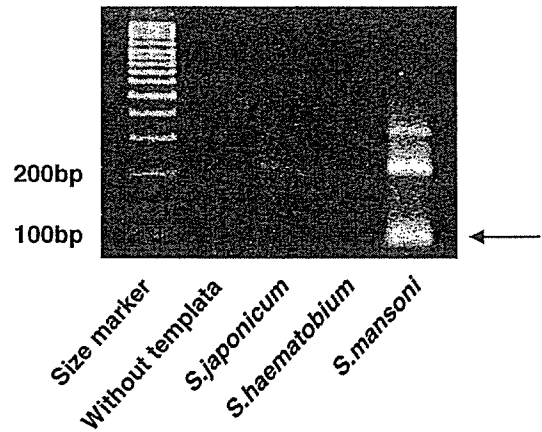


Fig. 2. Species-specificity of the touchdown PCR. One picogram of genomic DNA from each of three human schistosome species (*S. japonicum*, *S. haematobium* or *S. mansoni*) was amplified by the touchdown PCR. The size of the appropriate PCR products is indicated by an arrow on the right. The lengths of the size marker are indicated in b.p. on the left. Data representative of repeated experiments is shown.

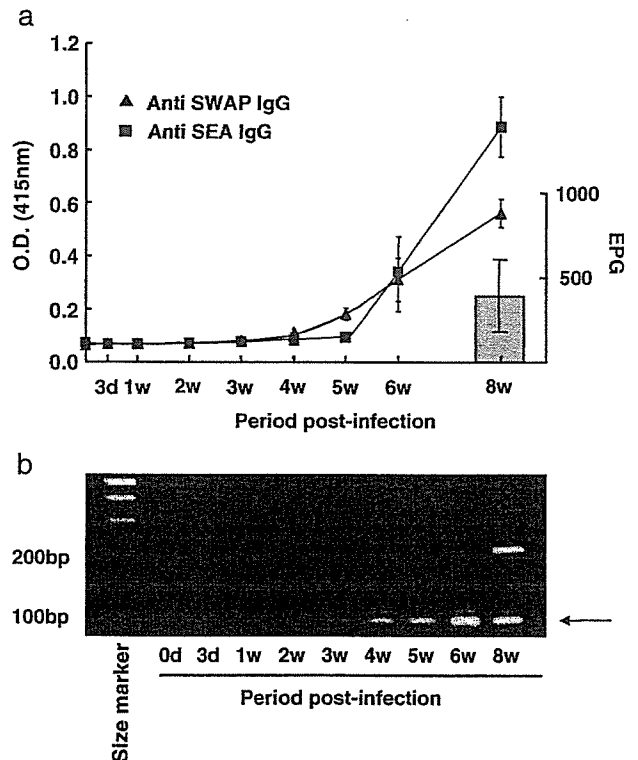


Fig. 3. Comparison of diagnostic potential in the early phase of infection between ELISA, stool examination and touchdown PCR. Serum samples and feces were collected before infection (0d), and at 3 days (3d) and at 1–8 weeks (1w–8w) post-infection. (a) Anti-schistosome IgG production and excretion of eggs into the feces. The values in line graphs represent the mean±standard deviation (S.D.) of IgG levels from four mice measured by ELISA. The values in the bar graph represent the mean±S.D. of EPG at 8 week post-infection. Up to 6week post-infection, no eggs were found in 20mg of the harvested feces (EPG<50). (b) Two microliters of pooled infected mouse serum was used directly as a template for the PCR amplification. The size of the appropriate PCR products is indicated by an arrow on the right. Data representative of repeated experiments is shown.

Table 2

The number of mice in which *S. mansoni* DNA was detected by the touchdown PCR

Period post-infection	3d	1w	2w	3w	4w	5w	6w	8w
PCR-positive mice/examined mice	0/4	0/4	3/4	2/4	3/4	3/4	4/4	4/4

when more than 10 fg of genomic DNA was used as a template (Fig. 1).

Although the dot blot for the target sequence showed an extremely stronger reaction to *S. mansoni* DNA than to *S. haematobium* DNA [20], it was not investigated whether only *S. mansoni* DNA was detected by the PCR. Therefore, the intra-genus species-specificity of the touchdown PCR was evaluated by amplifying 1 pg DNA of *S. japonicum*, *S. haematobium* and *S. mansoni* in the same condition. No PCR products were observed when *S. japonicum* DNA or *S. haematobium* DNA was used as a template (Fig. 2), indicating the absence of cross-reactive amplification of possible orthologous sequences in the two species. In addition, we did not find any false positive amplification bands when a normal mouse serum was applied to the PCR (corresponding to lane 0d in Fig. 3b).

3.2. Comparison of diagnostic potential between ELISA, stool examination and PCR

In order to compare the diagnostic potential of touchdown PCR with that of conventional techniques, we infected mice with 200 *S. mansoni* cercariae and periodically collected sera (for ELISA and PCR) and feces (for stool examination). As shown in Fig. 3a, anti-SWAP IgG and anti-SEA IgG were detected at 6 weeks post-infection. With the stool examination, no eggs were detected up to 6 weeks post-infection; i.e. EPG was <50. At 8 weeks, eggs were detected in the feces (Fig. 3a). The earliest egg deposition of eggs in the small intestines was observed at 5 weeks (data not shown).

In contrast to the diagnostic techniques above, we could observe a PCR product in the pooled serum at 2 weeks post-infection (Fig. 3b) and thereafter. The strength of the bands increased as the infection progressed. As shown in Table 2, we successfully detected *S. mansoni* DNA in more than or equal to half of the infected mice after 2 week post-infection.

4. Discussion

Schistosomiasis remains a serious world-wide health problem. The disease needs more sensitive and specific diagnostic methods. Such methods are required not only for people in endemic areas, but also increasingly for travelers who have become infected with the parasite during visits to such places. Diagnosis of the disease is usually based on the detection of parasite eggs by fecal examination or based on immunological methods. The fecal examination is simple, highly specific and cost-effective. Therefore, it is routinely used for epidemiological studies and for control programs in endemic areas [25,26]. However, it often misses light infections [7,27] and is not able to detect the infection until the parasite begins to

lay eggs. On the other hand, anti-schistosome antibody-based detection methods display a high sensitivity but not high specificity [28,29]. In our study, we also reconfirmed the inter-species cross-reactivity of ELISA. We checked the cross-reactivity of schistosome-infected mouse serum with each of three human-infecting schistosome antigens. *S. mansoni*-infected mouse serum (8 weeks post-infection) reacted with not only *S. mansoni* antigens (SWAP and SEA) but also antigens of *S. haematobium* and *S. japonicum* (data not shown). Similarly, *S. japonicum*-infected mouse serum (8 weeks post-infection) and *S. haematobium*-infected mouse serum (23 weeks post-infection) reacted with *S. mansoni* antigens (data not shown). Thus, as reported [29], ELISA with crude antigens had high levels of inter-species cross-reactivity. This fact makes it difficult to distinguish a *S. mansoni* infection from other schistosome infections by ELISA. In addition, the method is not able to detect the prepatent infection [30,31], and it is not easy to differentiate between acute and chronic schistosomiasis [23]. Several methods for detecting circulating schistosome antigens (CAA, CCA) have been reported [32,33]. These assays have both high sensitivity and high specificity, and can detect light infections. Notably, in the case of *S. haematobium* infection, one of these methods could easily detect the antigen in urine [34].

Recently, novel diagnostic methods based on PCR have been developed. The PCR assay is a sensitive and specific tool for the identification of cercariae in water [17,19] and of infected snails [18]. Pontes et al. reported the detection of *S. mansoni* DNA in human serum and feces [21]. They believed that the PCR assay might be a valuable alternative for the diagnosis of the disease. This new technique is expected to overcome the disadvantages of stool examinations and serological tests described above.

In this study, we confirmed the potential of the method described by Hamburger et al. Then, we tried to improve the technical procedures. We used a touchdown PCR, because spurious bands often appeared during amplification. Touchdown PCR was reported to make it possible to bypass spurious amplifications without lengthy optimization procedures [35]. In our experiments, the touchdown PCR swept away unexpected spurious bands. Additionally, this method enabled us to assay serum samples directly without having to extract DNA from them. In fact, 2 µl of serum is enough as a sample using our method. On the other hand, the method was still sensitive. It detected 10 fg of *S. mansoni* genomic DNA (Fig. 1). As regards its specificity, Hamburger et al. demonstrated that a probe for the 121-bp highly repeated sequence of *S. mansoni* did not react with *S. haematobium* DNA up to 100 ng using the dot blot technique [20] and Pontes et al. reported that the PCR product was observed when *S. mansoni* DNA was used for the template but was not observed when DNAs of other parasitic helminth were used [21]. However, the intra-genus species-specificity of the PCR has not been confirmed. In addition, the homologous sequences of the 121-bp tandem repeat from *S. mansoni* were shown to exist in the *S. haematobium* genome (*Dra*I) [19]. Although the sequence homology between *S. mansoni* and *S. haematobium* is not high, it is possible that PCR amplification would occur if *S. haematobium* DNA is used for the template.

Thus, we tested the species-specificity of the PCR. As shown in Fig. 2, we observed the appropriate PCR product only when *S. mansoni* DNA was used. No bands were observed when *S. japonicum* DNA or *S. haematobium* DNA was used as the template. This is the first demonstration of the intra-genus species-specificity of the PCR.

Next, experiments were carried out to clarify the potential value of our method as a diagnostic tool by using infected mice. For this purpose, we compared the PCR with conventional diagnostic techniques. We detected the eggs only at 8 weeks post-infection (Fig. 3a); i.e. no eggs were detected in the feces for up to 6 weeks. As this result may have been due to the low sensitivity of the stool examination, we also checked for the presence of eggs deposited in the digestive tract. The earliest deposition of eggs in the small intestines was observed at 5 weeks (data not shown). This is consistent with the fact that adult worms begin to lay eggs around 5 weeks suggesting that it is theoretically impossible to detect eggs in stool before 5 weeks. ELISA gave a positive result 6 weeks after the infection (Fig. 3a). Surprisingly, the PCR assay distinctly detected *S. mansoni* infection at 2 weeks, i.e. 3–6 weeks earlier than the other methods, in the mouse model.

The use of this PCR assay may make it possible to detect infections at an early stage of human cases. It is imperative to carry out further investigations using human sera. This PCR assay may prove a powerful tool for monitoring outbreaks in endemic areas and the early diagnosis of patients coming back from affected countries, although it demands special laboratory equipment when compared with fecal examinations and serological tests.

Acknowledgements

We are very grateful to Dr. Minoru Nomoto for technical advice and to Kyoko Masuda for assistance in the animal experiments. This work was supported financially by Grants-in-Aid from the Ministry of Health, Labor and Welfare of Japan (H15-Shinko-8), the US–Japan Cooperative Medical Science Program, and the Fukuoka Association of Medical Technologists.

References

- [1] Chitsulo L, Engels D, Montresor A, Savioli. The global status of schistosomiasis and its control. *Acta Trop* 2000;77:41–51.
- [2] Savioli L, Albonico M, Engels D, Montresor A. Progress in the prevention and control of schistosomiasis and soil-transmitted helminthiasis. *Parasitol Int* 2004;53:103–13.
- [3] Chen H, Lin D. The prevalence and control of schistosomiasis in Poyang Lake region, China. *Parasitol Int* 2004;53:115–25.
- [4] Whitty CJM, Mabey DC, Armstrong M, Wright SG, Chiodini PL. Presentation and outcome of 1107 cases of schistosomiasis from Africa diagnosed in a non-endemic country. *Trans R Soc Trop Med Hyg* 2000;94:531–4.
- [5] Day JH, Grant AD, Doherty JF, Chiodini PL, Wright SG. Schistosomiasis in travellers returning from sub-Saharan Africa. *Br Med J* 1996;313:268–9.
- [6] Hamilton JV, Klinkert M, Doenhoff MJ. Diagnosis of schistosomiasis: antibody detection, with notes on parasitological and antigen detection methods. *Parasitology* 1998;117:S41–57.
- [7] de Vals SJ, Gryseels B. Underestimation of *Schistosoma mansoni* prevalence. *Parasitol Today* 1992;8:274–7.
- [8] Doenhoff MJ, Chiodini PL, Hamilton JV. Specific and sensitive diagnosis of schistosome infection: can it be done with antibodies? *Trends Parasitol* 2004;20:35–9.
- [9] Imagawa DT, Lee MH, Wolinsky SM, et al. Human immunodeficiency virus type 1 infection in homosexual men who remain seronegative for prolonged periods. *N Eng J Med* 1989;320:1458–62.
- [10] Cloud JL, Carroll KC, Pixton P, Erali M, Hillyard DR. Detection of *Legionella* species in respiratory specimens using PCR with sequencing confirmation. *J Clin Microbiol* 2000;38:1709–12.
- [11] Eisenach KD, Cave MD, Bates JH, Crawford JT. Polymerase chain reaction amplification of a repetitive DNA sequence specific for *Mycobacterium tuberculosis*. *J Infect Dis* 1990;161:977–81.
- [12] Barker Jr RH, Banchongaksorn T, Courval JM, Suwonkerd W, Rimwungtragoon K, Wirth DF. A simple method to detect *Plasmodium falciparum* directly from blood samples using the polymerase chain reaction. *Am J Trop Hyg* 1992;46:416–26.
- [13] Sturm NR, Degraeve W, Morel C, Simpson L. Sensitive detection and schizodeme classification of *Trypanosoma cruzi* cells by amplification of kinetoplast minicircle DNA sequences: use in diagnosis of Chagas' disease. *Mol Biochem Parasitol* 1989;15(33):205–14.
- [14] de Bruijin MH, Barker DC. Diagnosis of new world leishmaniasis: specific detection of species of the *Leishmania braziliensis* complex by amplification of kinetoplast DNA. *Acta Trop* 1992;52:45–8.
- [15] Hanelt B, Adema CM, Mansour MH, Loker ES. Detection of *Schistosoma mansoni* in *Biomphalaria* using nested PCR. *J Parasitol* 1997;83:387–94.
- [16] Jannotti-Passos LK, Vidigal TH, Dias-Neto E, Pena SD, Simpson AJ, Dutra WO, et al. PCR amplification of the mitochondrial DNA minisatellite region to detect *Schistosoma mansoni* infection in *Biomphalaria glabrata* snails. *J Parasitol* 1997;83:395–9.
- [17] Hamburger J, Xu YX, Ramzy RM, Jourdane J, Ruppel A. Development and laboratory evaluation of a polymerase chain reaction for monitoring *Schistosoma mansoni* infestation of water. *Am J Trop Med Hyg* 1998;59:468–73.
- [18] Hamburger J, He-Na, Xu YX, Ramzy RM, Jourdane J, Ruppel A. A polymerase chain reaction assay for detecting snails infected with bilharzia parasites (*Schistosoma mansoni*) from very early prepatency. *Am J Trop Med Hyg* 1998;59:872–6.
- [19] Hamburger J, He-Na Abbasi I, Ramzy RM, Jourdane J, Ruppel A. Polymerase chain reaction assay based on a highly repeated sequence of *Schistosoma haematobium*: a potential tool for monitoring schistosome-infested water. *Am J Trop Med Hyg* 2001;65:907–11.
- [20] Hamburger J, Turetski T, Kapelle RI, Deresiewicz R. Highly repeated short DNA sequences in the genome of *Schistosoma mansoni* recognized by a species-specific probe. *Mol Biol Parasitol* 1991;44:73–80.
- [21] Pontes LA, Dias-Neto E, Rabello A. Detection by polymerase chain reaction of *Schistosoma mansoni* DNA in human serum and feces. *Am J Trop Med Hyg* 2002;66:157–62.
- [22] Osada Y, Kumagai T, Masuda K, Suzuki T, Kanazawa T. Mutagenicity evaluation of *Schistosoma* spp. extracts by the *umu*-test and V79/HGPRT gene mutation assay. *Parasitol Int* 2005;54:29–34.
- [23] Lunde MN, Ottesen EA, Cheever AW. Serological differences between acute and chronic *Schistosomiasis mansoni* detected by enzyme-linked immunosorbent assay (ELISA). *Am J Trop Med Hyg* 1979;28:87–91.
- [24] Sato Y, Toma H. *Strongyloides venezuelensis* infections in mice. *Int J Parasitol* 1990;20:57–62.
- [25] Katz N, Chaves A, Pellegrino J. A simple device for quantitative stool thick-smear technique in *Schistosomiasis mansoni*. *Rev Inst Med Trop Sao Paulo* 1972;14:397–400.
- [26] Bowie C, Purcell B, Shaba B, Makaula P, Perez M. A national survey of the prevalence of schistosomiasis and soil transmitted helminths in Malawi. *BMC Infect Dis* Nov 16 2004;4:49.
- [27] Engels D, Sinzinkayo E, Gryseels B. Day-to-day egg count fluctuation in *Schistosoma mansoni* infection and its operational implications. *Am J Trop Med Hyg* 1996;54:319–24.

- [28] Doenhoff MJ, Dunne DW, Lillywhite JE. Serology of *Schistosoma mansoni* infections after chemotherapy. *Trans R Soc Trop Med Hyg* 1989;83:237–8.
- [29] Doenhoff MJ, Butterworth AE, Hayes RJ, Sturrock RF, Ouma JH, Koech D, et al. Seroepidemiology and serodiagnosis of schistosomiasis in Kenya using crude and purified egg antigens of *Schistosoma mansoni* in ELISA. *Trans R Soc Trop Med Hyg* 1993;87:42–8.
- [30] Grobusch MP, Muhlberger N, Jelinek T, Bisoffi Z, Corachan M, Harms G, et al. Imported schistosomiasis in Europe: sentinel surveillance data from TropNetEurop. *J Travel Med* 2003;10:164–9.
- [31] Dunne DW, Bain J, Lillywhite J, Doenhoff MJ. The stage-, strain- and species-specificity of a *Schistosoma mansoni* egg antigen fraction (CEF6) with serodiagnostic potential. *Trans R Soc Trop Med Hyg* 1984;78:460–70.
- [32] de Jonge N, Kremsner PG, Krijger FW, Schommer G, Fillie YE, Cornelis D, et al. Detection of the schistosome circulating cathodic antigen by enzyme immunoassay using biotinylated monoclonal antibodies. *Trans R Soc Trop Med Hyg* 1990;84:815–8.
- [33] Attallah AM, Ismail H, El Masry SA, Rizk H, Handousa A, El Bendary M, et al. Rapid detection of a *Schistosoma mansoni* circulating antigen excreted in urine of infected individuals by using a monoclonal antibody. *J Clin Microbiol* 1999;37:354–7.
- [34] Al-Sherbiny MM, Osman AM, Hancock K, Deelder AM, Tsang VCW. Application of immunodiagnostic assays: detection of antibodies and circulating antigens in human schistosomiasis and correlation with clinical findings. *Am J Trop Med Hyg* 1999;60:960–6.
- [35] Don RH, Cox PT, Wainwright BJ, Baker K, Mattick JS. ‘Touchdown’ PCR to circumvent spurious priming during gene amplification. *Nucleic Acids Res* 1991;19:4008.

ANTIBODY ISOTYPE RESPONSES TO PARAMYOSIN, A VACCINE CANDIDATE FOR SCHISTOSOMIASIS, AND THEIR CORRELATIONS WITH RESISTANCE AND FIBROSIS IN PATIENTS INFECTED WITH *SCHISTOSOMA JAPONICUM* IN LEYTE, THE PHILIPPINES

TAKESHI NARA,* KYOICHI IIZUMI, HIROSHI OHMAE, ORLANDO S. SY, SOICHI TSUBOTA, YUTAKA INABA, AKIKO TSUBOUCHI, MASANOBU TANABE, SOMEI KOJIMA, AND TAKASHI AOKI

Department of Molecular and Cellular Parasitology and Department of Epidemiology and Environmental Health, Juntendo University School of Medicine, Tokyo, Japan; Laboratory of Imported Parasitic Diseases, Department of Parasitology, Institute of Infectious Diseases, Tokyo, Japan; Schistosomiasis Research Hospital, Palo, Leyte, The Philippines; Department of Tropical Medicine and Parasitology, School of Medicine, Keio University, Tokyo, Japan; Center for Medical Sciences, International University of Health and Welfare, Tochigi, Japan

Abstract. We examined whether antibody isotype responses to paramyosin (PM), a vaccine candidate for schistosomiasis, are associated with age-dependent resistance and pathology in liver fibrosis using human sera collected from 139 individuals infected with *Schistosoma japonicum* in Leyte, The Philippines. We report that IgA and IgG3 responses to PM showed a positive correlation with age and that the epitopes responsible were localized predominantly within the N-terminal half of PM. In addition, the IgG3 response to PM was associated with serum level of procollagen-III-peptide (P-III-P), an indicator of progression of liver fibrosis. These results imply that IgG3 against PM may not only provoke age-dependent resistance to *S. japonicum* infection but also enhance liver fibrosis. In contrast, levels of IgE to PM and to multiple PM fragments showed a negative correlation with P-III-P level. Thus, in contrast to IgG3, increases in PM-specific IgE may contribute to suppression of liver pathogenesis in schistosomiasis.

INTRODUCTION

A number of epidemiologic studies have suggested the occurrence of age-dependent, acquired resistance to reinfection with *Schistosoma mansoni*,¹ *S. haematobium*,² and *S. japonicum*.^{3,4} Age-dependent resistance is correlated with specific antibody isotype responses to the schistosome antigens, especially IgE responses to adult worm antigen (AWA).^{5–8} In addition, IgA specific to parasite antigens was shown to be associated with resistance.^{9,10} Thus, IgE and IgA may play a role in mediating protective immunity. Conversely, IgM, IgG2, and IgG4 have been suggested to block killing by antibody-dependent cellular cytotoxicity (ADCC) of the parasites, acting as a blocking antibody.^{6,11} Nevertheless, the responses of various isotypes are controversial in their ability to provoke an immune effector mechanism.

Paramyosin (PM) is an invertebrate myofibrillar protein and is one of six candidate vaccines against schistosomiasis.¹² Vaccination with recombinant PM induced a significant reduction in worm recovery after challenge infection with *S. japonicum* in mice, pigs, and water buffaloes as experimental animal models.^{13,14} Immunohistochemical and immunoelectron microscopic analyses indicated that PM is localized on the surface of cercaria, schistosomula, and adult *S. japonicum*, as well as in the muscle layers, suggesting that the surface PM could evoke ADCC.^{15,16} Passive transfer of PM-specific monoclonal IgE in mice at an early stage of challenge infection resulted in reduction of worm burden.¹⁷

In humans, antibody isotype responses against *S. japonicum* PM have been reported. A study in The Philippines showed that IgA titers to AWA are correlated with age and the major target of IgA was PM, suggesting a role of anti-PM IgA in acquired immunity.⁹ In contrast, antibody responses to

PM were not correlated with susceptibility in another study in China.¹⁸ These discrepancies may have been due to geographic differences of both human and parasite populations and differences in the PM epitopes recognized by the specific antibody isotypes, some of which would be protective with others acting as blocking antibodies.

The major pathologic lesion of *S. japonicum* infection is periportal fibrosis, which is a consequence of prolonged granuloma formation surrounding the deposited parasite eggs in the liver. From the practical view of vaccine development, schistosome vaccines are required not only to reduce worm burden but also to ameliorate liver fibrosis. With regard to the roles of isotype responses to parasite antigens in fibrosis, analyses of IgE-deficient mice infected with either *S. japonicum* or *S. mansoni* indicated that IgE modifies granuloma formation.^{19,20} In addition, increased levels of IgG4 to parasite egg antigens in schistosomiasis *mansoni* patients with and liver fibrosis have been demonstrated.²¹ Interestingly, PM has been suggested to be involved in granuloma formation in mice infected with *S. mansoni*.^{22,23} Thus, it is important to examine the role of isotype responses to PM in liver fibrosis for schistosome vaccine development.

The present study was performed to determine whether isotype responses against PM are involved in age-dependent resistance and liver fibrosis in human *S. japonicum* infection. We demonstrate that IgG3 and IgA against PM were correlated positively with age, and the epitopes recognized varied among isotypes. In addition, we observed a positive correlation between IgG3 responses to PM and serum level of procollagen-III-peptide (P-III-P), an indicator of progression of liver fibrosis. Surprisingly, IgE specific to PM showed a negative correlation with P-III-P level, suggesting the involvement of IgE-PM interactions in liver fibrosis. The possibility of using PM as a schistosome vaccine is also discussed.

MATERIALS AND METHODS

Study design and evaluation of liver fibrosis. The study was carried out in villages in Leyte, The Philippines, where schis-

* Address correspondence to Takeshi Nara, Department of Molecular and Cellular Parasitology, Juntendo University School of Medicine, Hongo 2-1-1, Bunkyo-ku, Tokyo 113-8421, Japan. E-mail: tnara@med.juntendo.ac.jp

tosomiasis japonica is endemic. In this area, mass screening by semi-quantitative stool examination using Kato-Katz method, followed by treatment with praziquantel against *S. japonicum* infection, was conducted from 1981 to 1999, as part of the National Schistosomiasis Control Program of the Philippines. In July and August 1999, outpatients from Schistosomiasis Research Hospital, who were diagnosed as having *S. japonicum* infection by detection of the parasite eggs in their feces, were enrolled in the present study. The purpose and protocols of the study were explained and written consent obtained from all the patients. All enrolled patients underwent serologic and ultrasonographic examinations. Patients positive for hepatitis B surface antigen by radioimmunoassay (cut-off index > 2.0) and/or antibody to hepatitis C virus (second generation) and persons with alcoholism with bright liver by ultrasonography (alcohol consumption > 80 mL/day for \geq 5 years) were excluded from the study.

A total of 139 patients were selected for further analyses. The degree of liver fibrosis was estimated by ultrasonography and classified into four stages (type 0: normal pattern; type 1: linear pattern; type 2: tubular pattern; type 3: Network pattern) as described.^{24,25} Serum levels of P-III-P, type IV collagen, and total bile acids (TBAs) were measured in only 133 of the 139 blood specimens because the other six specimens were lost during analyses. Eight control sera were collected from healthy adult volunteers who lived in Japan and were free from *S. japonicum* infection.

Schistosome antigens and recombinant paramyosins. Soluble AWA was extracted from adult worms of the Yamanashi strain of *S. japonicum* by repeated freezing and thawing.¹⁷ After centrifugation at $10,000 \times g$ for 30 minutes at 4°C, the supernatant was recovered and cryopreserved at -80°C until use. Full-length *S. japonicum* PM and six truncated forms were designated as PM (1–866 amino acids), PM1 (1–164 amino acids), PM2 (157–302 amino acids), PM3 (297–451 amino acids), PM4 (447–602 amino acids), PM5 (597–742 amino acids), and PM6 (734–866 amino acids). The PM cDNAs were amplified by a polymerase chain reaction using the *S. japonicum* PM cDNA¹⁶ as a template and the following primers: PM, 5'-CGGGATCCCATATGATGAATCACGATACAG-3' and 5'-GCGGATCCTACATCATACTTGTTGC-3'; PM1, 5'-CGGGATCCCATATGATGAATCACGATACAG-3' and 5'-CGGGATCCCGGGTACCGAGCTCGACTTTTGATTGAGCTGATTG-3'; PM2, 5'-CGGGATCCCATATGGTTCGACGAATTCGCTAAGCAATCAGCTGAATC-3' and 5'-CGGGATCCCTCGAGAAGCTTGAATTCCTCTGTTTTACTC-3'; PM3, 5'-CGGGATCCGAGTAAACAAGAGGAATTC-3' and 5'-CGGGATCCCGACTTCTAATTGAGACCA-3'; PM4, 5'-CGGGATCCGCTCTCAATTAGGAAGCTGAA-3' and 5'-CGGGATCCCAACTTCATTTGCCAGCTG-3'. The amplified cDNAs were digested with *Nde* I/*Bam* HI (PM, PM1, and PM2) or *Bam* HI (PM3 and PM4) and subcloned into the expression vector pET14b. cDNA for PM5 was derived by *Pvu* II/*Eco* RI digestion of the PM cDNA, end-filled, and subcloned into the *Eco* RV site of the pT7Blue-T vector (Novagen Inc., Madison, WI). The *Nde* I/*Bam* HI fragment carrying the PM5 cDNA was subcloned into pET14b. The cDNA of PM6 was derived by *Pst* I/*Bam* HI digestion of the PM cDNA, end-filled, and subcloned into the end-filled *Xho* I site of pET14b. Transformation of bacteria, induction of expression, and purification of recombinant PMs with an N-

terminal histidine 6-tag were carried out as described.¹³ The PM was found to contain many degraded forms and was purified further by sodium dodecyl sulfate–polyacrylamide gel electrophoresis, followed by electro-elution. The recombinant PMs were stored in 10 mM sodium phosphate (pH 7.2), 1 M NaCl, and 4 M urea at -80°C until use.

Measurement of antibody titer specific to the schistosome antigens in human sera. An enzyme-linked immunosorbent assay (ELISA) was carried out using AWA, the full-length PM, and a series of recombinant PMs. Briefly, 96-well microtiter plates were coated with 5 μ g/ml of AWA or 1 μ g/ml of PMs. After washing out the unbound antigens three times with phosphate-buffered saline (PBS) containing 0.05% Tween 20 (PBST), the plates were blocked with blocking solution containing 0.5% bovine serum albumin (fraction V; Sigma Chemical Co., St. Louis, MO) in PBST for 30 minutes at room temperature. The plates were then washed three times with PBST. Human sera were diluted 1:100 with blocking solution for detection of IgG, IgG1, IgG2, and IgG3 and 1:50 for detection of IgG4, IgE, and IgA, and then incubated overnight at 4°C. The plates were washed five times with PBST and incubated with horseradish peroxidase-conjugated anti-human IgG1, IgG2, IgG3, IgG4, and IgA (anti-IgG; EY Laboratories, Inc., San Mateo, CA; IgG1, IgG2, IgG3, and IgG4; Southern Biotechnology Associates Inc., Birmingham, AL; and IgA; ICN Biomedicals, Costa Mesa, CA) or biotinylated anti-human IgE (Vector Laboratories Inc., Burlingame, CA) at a dilution of 1:1,000 for one hour at room temperature. The plates were then washed five times with PBST. For detection of IgE, the plates were further treated with a VECTASTAIN® Elite ABC standard kit under the conditions recommended by the manufacturer (Vector Laboratories Inc.). The assays were developed with 2,2'-azino-bis(3-ethylbenzthiazoline-6-sulfonic acid) and the optical density was measured at 405 nm using a microplate reader (Model MTP-22; Corona Electrics Co. Ltd., Ibaraki, Japan) with a reference measured at 492 nm.

Statistical analysis. StatView™ version 4.0 (Abacus Concepts Inc., Berkeley, CA) and HALWIN version 6.2 (Gendai-Sugakusha Co. Ltd., Kyoto, Japan) were used for data analyses. Optical densities of serum concentrations of P-III-P and type IV collagen and the antibody titers were log-transformed before analyses. We used Student's *t*-test to evaluate differences of log-transformed means of antibody titers between the study and control groups. Pearson's correlation coefficient was used to quantify associations between age, ultrasonographic evaluation, and log-transformed data for P-III-P, type IV collagen, and antibody titers. In the present study, no correction has been made for multiple comparisons between levels of antibodies to AWA and PM in correlation analyses with epidemiologic indicators because PM is present in the AWA preparation and, therefore, anti-AWA responses include the responses to PM. Multiple regression analysis was used for comparisons of isotype response levels against the PM fragments and their correlations with age and markers of fibrosis.

RESULTS

Epidemiologic outcomes. The cohort of 139 subjects ranged in age from 9 to 69 years old, and the male:female sex ratio was 92:47. Table 1 shows the relationships between age

TABLE 1
Correlations between age and markers of fibrosis in schistosomiasis japonica patients in Leyte, The Philippines*

Markers	Correlation coefficient (<i>R</i>)		
	US score	P-III-P†	Type IV†
Age	0.488 (< 0.001)	0.039 (0.655)	0.126 (0.147)
US score		0.306 (0.003)	0.278 (0.001)
P-III-P			0.670 (< 0.001)

* US = ultrasound. Values in parentheses are *P* values.
† Transformed into log₁₀.

and markers of fibrosis in our patient population. We adopted four indicators to estimate the degree of liver fibrosis: ultrasonographic score and serum levels of P-III-P, type IV collagen, and TBA.

Age showed a strong correlation with ultrasonographic score ($R = 0.488$, $P < 0.001$), but was not correlated with P-III-P or type IV collagen levels. In addition, ultrasonographic score was correlated with P-III-P and type IV collagen levels ($R = 0.306$, $P = 0.003$ and $R = 0.278$, $P = 0.011$, respectively). In contrast, the TBA level was not correlated with age, ultrasonographic score, or other serologic markers.

Relationships between age and antibody isotype responses against PM. To determine whether isotype responses against PM are associated with age-dependent resistance in Filipino patients, we measured the serum levels of IgA, IgE, IgG1, IgG2, IgG3, and IgG4 against PM and AWA (Figure 1). Because the reactivity of secondary antibodies used for the ELISA varied, it was difficult to determine the amounts of antibody among the isotypes. With the exception of IgG2, the levels of all antibody isotypes against PM and AWA increased significantly in patients infected with *S. japonicum*. The unresponsiveness of IgG2 production against AWA in Filipino patients was consistent with previous findings in Chinese patients with schistosomiasis japonica.¹⁸

We selected IgA, IgE, IgG1, IgG3, and IgG4 isotypes to examine the relationships between age and their responses against AWA and PM (Table 2). Age showed a positive correlation with serum levels of IgG3 against both AWA ($R = 0.216$, $P = 0.014$) and PM ($R = 0.325$, $P = 0.001$) and with

the level of IgA against PM ($R = 0.226$, $P = 0.007$). This was in part consistent with the findings of a previous report, in which the anti-AWA IgA level was correlated with age and PM was a major target of the IgA response in The Philippines.⁹ The IgE, IgG1, and IgG4 responses did not show such correlations with age.

Relationships between fibrosis and antibody isotype responses against PM. To determine whether isotype response levels against PM are associated with fibrosis, we examined the relationships between fibrosis and levels of IgA, IgE, IgG1, IgG3, and IgG4 against PM in patients with schistosomiasis japonica. We observed that correlations of isotype responses with fibrosis were different among the indicators of fibrosis, ultrasonographic score and serum levels of P-III-P and type IV collagen (Table 3). With ultrasonographic score, positive correlations were observed for IgA, IgG3, and IgG4 levels against PM. In contrast, the P-III-P level showed a positive correlation only with IgG3 to PM, and type IV collagen level was not associated with isotype responses to PM.

Unexpectedly, IgE levels against PM showed a negative correlation with serum P-III-P level ($R = -0.260$, $P = 0.003$; Table 3), in which individuals with high IgE titers developed lower levels of serum P-III-P. Such trends were also observed between ultrasonographic score and level of IgE to PM ($R = -0.069$, $P = 0.441$), and between type IV collagen and IgE levels ($R = -0.107$, $P = 0.228$).

The IgG1 responses to AWA showed a positive correlation with the ultrasonographic score ($R = 0.320$, $P < 0.001$), but no positive correlations were observed against PM. These results suggest that fibrosis associated with IgG1 responses may be attributable to other parasite antigens.

Epitope analyses of PM recognized by isotypes. In light of these findings, we attempted to identify the epitopes recognized by IgA, IgE, IgG3, and IgG4 isotypes that are associated with age-dependent resistance or fibrosis in *S. japonicum* infection. We constructed a series of deletion mutants, PM1 (1–164 amino acids), PM2 (157–302 amino acids), PM3 (297–451 amino acids), PM4 (447–602 amino acids), PM5 (597–742 amino acids), and PM6 (734–866 amino acids). These truncated mutants had an average length of 150 amino acids and provided a sequential overlap of at least five residues (Figure 2).

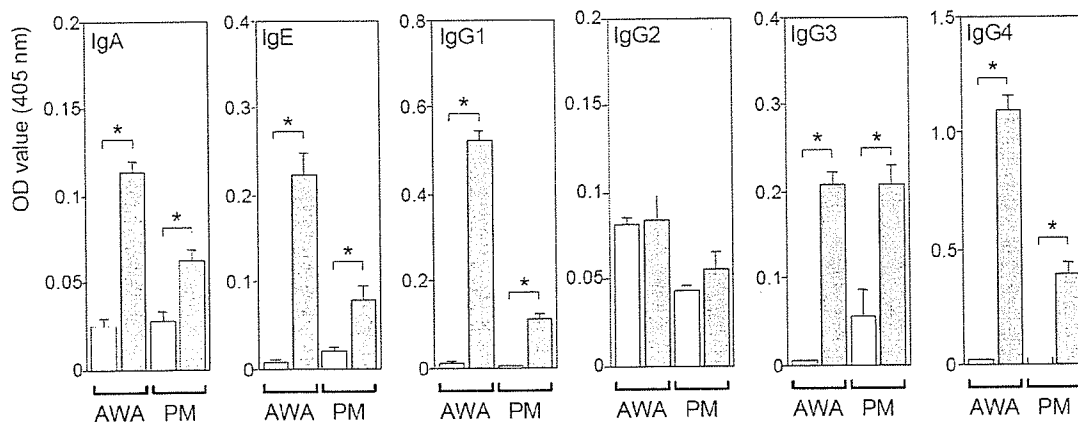


FIGURE 1. Antibody isotype levels (geometric mean \pm SE) against *Schistosoma japonicum* adult worm antigens (AWA) and paramyosin (PM) in 8 healthy (open bars) and 139 infected (gray bars) individuals OD = optical density. * $P < 0.01$.

TABLE 2
Correlations between antibody isotype levels (\log_{10}) to *Schistosoma japonicum* antigens and age*

Antibody	Correlation coefficient (<i>R</i>) by antigen							
	AWA	PM	PM1	PM2	PM3	PM4	PM5	PM6
IgA	0.138 (0.105)	0.226 (0.007)	0.150 (0.077)	0.234 (0.006)	0.335 (< 0.001)	0.117 (0.169)	0.113 (0.185)	0.004 (0.966)
IgE	-0.064 (0.473)	0.031 (0.731)	0.113 (0.204)	0.041 (0.648)	-0.004 (0.964)	-0.060 (0.502)	-0.027 (0.762)	0.016 (0.360)
IgG1	0.093 (0.287)	0.113 (0.198)						
IgG3	0.216 (0.014)	0.325 (< 0.001)	0.268 (0.002)	0.254 (0.003)	0.183 (0.037)	0.030 (0.733)	0.223 (0.011)	0.090 (0.307)
IgG4	0.092 (0.306)	0.152 (0.088)	0.126 (0.158)	0.108 (0.226)	0.231 (0.009)	0.114 (0.201)	0.239 (0.007)	0.084 (0.346)

* Values in parentheses are *P* values. *R* values for IgG1 responses to the truncated PMs are not shown. AWA = adult worm antigen; PM = paramyosin.

Box and whisker plots of isotype responses demonstrated the presence of low responders and high responders for antibody production against the full-length PM and its deletion mutants (Figure 3). Among the deletion mutants, PM6 hardly evoked any antibody production for any antibody isotype. The IgA and IgG3 isotypes reacted predominantly with the PM1, PM2, and PM3 mutants. In contrast, IgG4 appeared to react predominantly with PM2, PM3, PM4, and PM5. IgE did not show such specificity.

The IgA and IgG3 response levels against PM1, PM2, and

PM3, and IgG3 levels against PM5 showed a positive correlation with age (Table 2). Multiple regression analysis was carried out to specify the responsible PM epitope(s) and showed correlations of age with IgA levels against PM3 ($R = 0.356$, $P < 0.001$) and with IgG3 levels against PM2 and PM3 ($R = 0.318$, $P < 0.001$ and $R = 0.307$, $P < 0.001$, respectively). These results suggest that levels of anti-PM3 IgA and levels of anti-PM2 and anti-PM3 IgG3 are likely to be associated with age-dependent resistance.

With regard to fibrosis, IgG3 levels against any of the de-

TABLE 3
Correlations between antibody isotype levels (\log_{10}) to antigens of *Schistosoma japonicum* and various markers of fibrosis*

Antibody	Correlation coefficient (<i>R</i>) by antigen							
	AWA	PM	PM1	PM2	PM3	PM4	PM5	PM6
US score								
IgA	0.143 (0.094)	0.180 (0.034)	0.109 (0.204)	0.280 (< 0.001)	0.180 (0.034)	0.128 (0.134)	0.124 (0.146)	0.111 (0.193)
IgE	0.035 (0.693)	-0.069 (0.441)	0.031 (0.726)	-0.020 (0.821)	-0.111 (0.210)	-0.124 (0.163)	-0.130 (0.141)	-0.204 (0.020)
IgG1	0.320 (< 0.001)	0.081 (0.352)						
IgG3	0.313 (< 0.001)	0.241 (0.006)	0.017 (0.845)	0.151 (0.086)	0.156 (0.076)	0.084 (0.344)	0.142 (0.107)	-0.084 (0.344)
IgG4	0.198 (0.026)	0.246 (0.005)	0.196 (0.027)	0.137 (0.124)	0.106 (0.235)	0.186 (0.186)	0.256 (0.004)	0.128 (0.151)
P-III-P								
IgA	0.027 (0.756)	-0.048 (0.587)	-0.025 (0.77)	0.263 (0.002)	0.194 (0.025)	-0.013 (0.880)	0.295 (< 0.001)	0.238 (0.006)
IgE	-0.049 (0.581)	-0.260 (0.003)	0.051 (0.564)	-0.056 (0.531)	-0.178 (0.043)	-0.304 (< 0.001)	-0.260 (0.003)	-0.194 (0.027)
IgG1	0.097 (0.267)	-0.156 (0.074)						
IgG3	0.215 (0.014)	0.292 (< 0.001)	0.025 (0.776)	0.188 (0.033)	0.216 (0.014)	0.011 (0.900)	0.286 (< 0.001)	0.182 (0.038)
IgG4	0.028 (0.751)	0.076 (0.397)	0.120 (0.178)	0.056 (0.532)	0.025 (0.777)	0.028 (0.755)	0.085 (0.342)	0.085 (0.342)
Type IV								
IgA	-0.079 (0.306)	-0.067 (0.447)	0.032 (0.719)	0.038 (0.666)	-0.014 (0.869)	0.027 (0.755)	0.088 (0.316)	0.084 (0.337)
IgE	-0.030 (0.734)	-0.107 (0.228)	-0.041 (0.645)	-0.093 (0.296)	-0.062 (0.488)	-0.140 (0.114)	-0.072 (0.416)	0.002 (0.978)
IgG1	0.072 (0.413)	-0.057 (0.514)						
IgG3	0.174 (0.047)	0.150 (0.088)	0.073 (0.413)	0.053 (0.551)	0.020 (0.825)	-0.037 (0.675)	0.088 (0.321)	0.177 (0.044)
IgG4	-0.032 (0.719)	-0.035 (0.693)	0.100 (0.266)	-0.031 (0.731)	-0.034 (0.706)	-0.007 (0.940)	0.032 (0.718)	-0.013 (0.884)

* Values in parentheses are *P* values. *R* values for IgG1 responses to the truncated PMs are not shown. US = ultrasound; AWA = adult worm antigen; PM = paramyosin.